© [2014]

Sarah Hassanien

ALL RIGHTS RESERVED

CHARACTERIZATION OF THE NOVEL H82R MUTATION IN CGI-58 THAT CAUSES NEUTRAL LIPID STORAGE DISORDER IN HUMANS

By

SARAH HASSANIEN

A thesis submitted to the

Graduate School-New Brunswick

Rutgers, The State University of New Jersey

in partial fulfillment of the requirements

for the degree of

Master of Science

Graduate Program in Nutritional Sciences

written under the direction of

Dr. Dawn L. Brasaemle

And approved by

_____

_____

_____

New Brunswick, New Jersey

October 2014

ABSTRACT OF THE THESIS

Characterization of the novel H82R mutation in CGI-58 that causes Neutral Lipid Storage Disorder in humans

By SARAH HASSANIEN

Thesis Director:

Dr. Dawn L. Brasaemle

Comparative gene identification-58 (CGI-58) interacts with and co-activates adipose triglyceride lipase (ATGL). The H82R mutation in human CGI-58 causes a neutral lipid storage disorder (NLSD) characterized by ichthyosis and excessive triacylglycerol storage in many types of cells. We studied the comparable H84R mutation in mouse CGI-58, and H84A mutated CGI-58, to ask how CGI-58 function is impaired. The ectopic expression of wild-type (WT) CGI-58 in human NLSD fibroblasts reduced excessive triglyceride storage to normal levels, whereas H84R CGI-58 was ineffective. Additionally, H84R CGI-58 failed to co-activate ATGL in an *in vitro* triglyceride hydrolase assay and H84A CGI-58 was not as efficient, when compared to WT CGI-58. Immunofluorescence microscopy revealed that H84R and H84A CGI-58 localized to ectopic perilipin 1A on lipid droplets of cultured NIH3T3CARΔ fibroblasts as well as WT CGI-58. Moreover, the addition of forskolin and isobutylmethylxanthine to the cells triggered the dispersion of all three variants of CGI-58 from the perilipin scaffold into the cytoplasm. A co-immunoprecipitation assay demonstrated that H84R and H84A CGI-58 bound ATGL as well as WT CGI-58. Additionally, while WT CGI-58 and ATGL can be

individually recruited to lipid droplets and ATGL recruitment to lipid droplets is increased in the presence of CGI-58, the H84R and H82R mutations do not interfere with lipid droplet recruitment of CGI-58 with ATGL. Thus, although H84R CGI-58 shows appropriate subcellular localization in cells expressing perilipin 1A, binds to ATGL, and is effectively recruited to lipid droplets, it does not co-activate ATGL's hydrolase activity. Future experiments are needed to explore additional mechanisms for deficient function of H84R CGI-58.

ACKNOWLEDGMENTS

I offer my sincere gratitude to my advisor and mentor, Dr. Dawn Brasaemle. Thank you for your guidance and motivation throughout this research project. The immense amount of knowledge that I have gained during the past two years is so valuable to me. I am also thankful for your support during what was arguably the most stressful, yet most important time of my life. I would like to acknowledge and thank my committee members, Dr. Judith Storch and Dr. Tracy Anthony, for their advice, encouragement, and support. I would also like to thank Dr. Laura Listenberger for sharing her lipid droplet binding assay protocol and assisting me in designing an ideal experiment.

I have to immensely thank my co-worker, Anna Dinh, without whom I would not be completing my thesis. This goes without saying, but thank you for helping me with every single one of my experiments, even with snack breaks every 5 minutes. Offering you cookies in exchange for help in the lab is easily the best business deal I ever made. Joking and laughing with you every day is what encouraged me to push forward and gaining you as a friend is possibly the most rewarding byproduct of this experience.

I want to thank past members of our lab for their contributions to my project: Dr. Derek McMahon, Dharika Shah, and Anita Sahu. From our lab, I would like to specifically thank Mayda Hernandez for her laughs, advice, and continuous friendship, and Daniel Kurz for his time and effort on the CGI-58 model. I have had the pleasure of working with the intelligent and talented undergraduates Lauren Simon and Brittney Suchan. Thank you both for maintaining an efficient workspace, helping with my experiments, and being great company. I have made such incredible friends here at Rutgers, who have offered me such great advice and are always there for a much needed

vent session. Many thanks to Lindsey Phillipson-Weiner, Dr. Angela Gajda, Juliet Gotthardt, Marc Tuazon, and Het Desai. I would like to specially thank Lindsey for being such a supportive friend and always making me laugh; I can always count on her to revive the lab with her animated singing (Disney tunes)! I am also incredibly blessed with the greatest friends; thank you Dalia, Dinah, Nadya, and Rania for always being there for me and never letting me quit.

Finally, I'd like to thank my caring and supportive family that I love with all my heart. I am in debt to my parents for providing me with endless opportunities to better myself and supporting any and all of my life decisions. Thank you to my 2 younger brothers, Omar and Yousef, for innocently making graduate school way more stressful than it had to be, and by doing so, making me a much stronger person. I would like to whole-heartedly thank my husband, Omar. This is not only my accomplishment, but yours as well. Thank you for believing in me when I felt hopeless and jaded, inspiring me to be the best I can be, and being the light at the end of my tunnel. I love you deeply.

TABLE OF CONTENTS

Page

LIST OF FIGURES

Figure Page

LIST OF ABBREVIATIONS

ABHD5 – α/β-hydrolase domain-containing protein 5

AMPK – 5' adenosine monophosphate-activated protein kinase

ATGL – Adipose triglyceride lipase

BSA – Bovine serum albumin

cAMP – Cyclic adenosine monophosphate

CAR – Coxsackie and adenovirus receptor

CGI-58 – Comparative Gene Identification 58

DAG – Diacylglycerol

DMEM – Dulbecco's modified Eagle medium

DTT – Dithiothreitol

EDTA – Ethylenediaminetetraacetic acid

FAF BSA – Fatty acid-free bovine serum albumin

G418 – Geneticin

GOS2 – G_0/G_1 switch gene 2

HCl – Hydrogen chloride

HSL – Hormone sensitive lipase

IBMX – 3-isobutyl-1-methylxanthine

IPTG – Isopropyl β-D-1-thiogalactopyranoside

IgG – Immunoglobulin G

KCl – Potassium chloride

LB – Luria broth

LD – Lipid droplet

LSB – Laemmli sample buffer

MAG – Monoacylglycerol

MGL – Monoglyceride lipase

NaCl – Sodium chloride

NaF – Sodium fluoride

NLSD – Neutral lipid storage disorder

NP-40 – Nonidet P-40

PAGE –Polyacrylamide gel electrophoresis

PBS – Phosphate buffered saline

PC – Phosphatidylcholine

PI – Phosphatidylinositol

PKA – Protein kinase A

PLIN1 – Perilipin 1A

SDS – Sodium dodecyl sulfate

TAG – Triacylglycerol

TIP47 – Tail-interacting protein of 47 kDa

TBST – Tris buffered saline with Tween-20

WT – Wild-type

INTRODUCTION

Obesity is a multi-faceted problem that is currently a nationwide epidemic. According to the Centers for Disease Control and Prevention (CDC), over one third of American adults were obese in 2011-2012 (1). Obesity is most commonly defined by a body mass index (BMI) greater than or equal to 30 and is due to disproportionate caloric intake, sedentary life-style or lack of exercise, and sometimes even genetics. Many health risks are associated with obesity including type 2 diabetes mellitus, coronary heart disease, hypertension, and other chronic diseases (2). Generally, obese people consume more calories than they utilize, which causes an energy imbalance. These excess calories are stored in the form of triacylglycerol (TAG) within adipose tissue. Studying the regulation of TAG homeostasis, including lipogenesis and intracellular lipolysis, or the breakdown of lipids, is essential to understanding factors that contribute to obesity.

Adipose tissue serves as an energy storage depot. Within adipose tissue, cells called adipocytes are the major sites of TAG storage in the body. TAGs are composed of three fatty acids esterified to a glycerol backbone. Adipocytes store TAG within lipid droplets, but also release fatty acids from the hydrolysis of TAGs when energy is needed. Lipid droplets (LDs) have a hydrophobic core containing neutral lipids, such as TAGs, diacylglycerols (DAG), and cholesterol esters, surrounded by a phospholipid monolayer, which also contains cholesterol (3). This phospholipid monolayer allows the LDs to exist in the aqueous environment of the cell as well as providing a surface with which proteins can interact (4). Specialized proteins called lipases can embed into the monolayer and hydrolyze the lipids in the cores of LDs.

In adipocytes, lipolysis requires three enzymes for full hydrolysis of TAG: desnutrin/adipose triglyceride lipase (ATGL), hormone-sensitive lipase (HSL), and monoacylglycerol lipase (MGL) (5). Hormones, specifically insulin and catecholamines, regulate lipolysis in adipocytes. During basal conditions, or the fed state, binding of insulin to the insulin receptor produces tyrosine phosphorylation of the receptor that initiates a signaling cascade that activates phosphodiesterases. Phosphodiesterases catalyze the breakdown of cyclic adenosine monophosphate (cAMP) to its inactive form, which results in reduced activation of protein kinase A (PKA); these conditions reduce lipolysis and promote TAG storage (6). When energy is needed by the body, catecholamines from systemic circulation and the sympathetic nervous system bind G-protein-coupled β-adrenergic receptors on the plasma membranes of adipocytes, leading to the activation of adenylyl cyclase. Adenylyl cyclase catalyzes the conversion of ATP into cAMP, subsequently promoting the activation of PKA-mediated phosphorylation events and ultimately leading to increases in lipolysis. (7,8).

In times of energy use or deprivation and starvation, the hydrolysis of TAG results in the release of three molecules of fatty acids and one molecule of glycerol into circulation. Fatty acids released from the lipolysis of adipose TAG stores can be either re-esterified into TAG and packaged into LDs or released into the bloodstream bound to albumin, delivered to peripheral tissues, and used as substrates for energy production (9). A defect in the process of lipid turnover can result in an accumulation of TAG, leading to obesity and its associated health risks. Dysregulation of lipid homeostasis can also have detrimental metabolic and phenotypic effects independent of obesity. For example, patients with Neutral Lipid Storage Disorder (NLSD) have increased TAG storage in

cells that usually do not store much TAG, such as keratinocytes and neutrophils, yet these individuals are not obese (10). One form of this disorder is caused by mutations in the gene encoding Comparative Gene Identification-58 (CGI-58), a protein that co-activates the major adipose TAG lipase, ATGL (11,12). The present work investigates an uncharacterized mutation in CGI-58 responsible for NLSD with the purpose of gaining understanding of the function of CGI-58 and its role in lipid homeostasis.

Perilipin 1A

In 1991, perilipin 1 (PLIN1) was discovered on LDs isolated from rat epididymal adipocytes (13). PLIN1 is the first protein of the perilipin family to be identified; four other members of the protein family were subsequently discovered, including adipophilin or adipose differentiation-related protein (PLIN2), tail-interacting protein 47 (PLIN3), S2-12 (PLIN4), and OXPAT (PLIN5) (14–17). Expression of PLIN1 is highest in adipocytes of white adipose tissue (WAT) and brown adipose tissue (BAT), but it is also expressed at lower levels in steroidogenic cells; in both types of cells it is localized exclusively to LDs (4,13,18,19).

In 2000, Brasaemle *et al.* showed that cells ectopically expressing PLIN1 accumulate TAG due to reduced TAG turnover (18). At the time, these researchers hypothesized that PLIN1 shields stored TAG from lipase-mediated hydrolysis (18). Additionally, PLIN1-null mice (PLIN $^{-/-}$) were generated by two groups to study the function of PLIN1 (20,21). PLIN $^{-/-}$ mice were lean, and had reduced fat mass and an increased metabolic rate when compared to WT mice (20,21). Adipocytes isolated from these mice showed higher levels of basal lipolysis that was most likely due to the reduced barrier to lipolysis on LDs caused by the substitution of PLIN2 for PLIN1 on LDs (21).

These observations are consistent with the cell experiments showing that PLIN1 protects LDs from lipolysis under basal conditions. Moreover, the protein is thought to not only restrict the access of lipases to their substrates under basal or fed conditions, but also to facilitate lipolysis by multiple mechanisms when energy is needed by the body (18,22). Under lipolytically stimulated conditions, PKA phosphorylates mouse PLIN1 on at least 6 serine residues, suggesting that PLIN1 is a major regulator of lipolysis. Phosphorylation of 3 amino-terminal serine residues in PKA sites increases lipolysis by HSL, whereas phosphorylation of 3 carboxy-terminal serine residues in PKA sites is important for ATGL-mediated lipolysis (23–25). In 2004, Brasaemle and co-workers hypothesized that PLIN1 serves as a scaffold at the surfaces of LDs to coordinate the access of lipid metabolic enzymes to LDs (26). This 2004 study and subsequent studies have revealed that different proteins bind to the PLIN1 scaffold under basal and stimulated conditions.

Hormone-Sensitive Lipase.

HSL was the first and most studied neutral lipid lipase identified in adipocytes. HSL is highly expressed in adipocytes of WAT and BAT, and to a lesser extent in steroidogenic cells, pancreatic β-cells, macrophages, and heart and skeletal muscle (27–32). HSL has been shown to hydrolyze multiple substrates *in vitro*, supporting the hypothesis that it is the major TAG and DAG lipase in adipocytes (33,34). However, DAG is likely the preferred substrate since HSL hydrolyzes DAG at a 10-fold higher rate than either TAG or MAG *in vitro* (35).

HSL is regulated by hormonal stimuli and is a substrate for 5’ adenosine monophosphate-activated protein kinase (AMPK) and PKA. Under basal conditions, high insulin levels lead to an increase in phosphodiesterase activity, which subsequently

causes a decrease in cAMP levels and PKA activity (36,37). Under these conditions, HSL is primarily phosphorylated by AMPK on serine residue 565 (of rat HSL) and results in the inactivation of the lipase while promoting cytosolic localization (38–40). Ser565 is dephosphorylated when PKA-mediated phosphorylation of neighboring ser563 occurs under lipolytically stimulated conditions (41). When catecholamines bind to β-adrenergic receptors, PKA-mediated phosphorylation of HSL activates the lipase, promoting the translocation of the protein from the cytosol to the surfaces of LDs where it gains access to its neutral lipid substrates (23,24,41,42). Additionally, the phosphorylation of the amino-terminal serine residues of PLIN1 facilitates HSL docking on the LD through a protein-protein interaction with PLIN1 (23,24).

To study the physiological function of HSL, several research groups have made whole-body HSL knockout mice (35,43,44). To everyone's surprise, these knockout mice were not obese, indicating that HSL is not the only TAG lipase in adipocytes. Adipose lipolysis was only mildly impaired (35). HSL's function as a major DAG lipase was revealed when the mice exhibited an accumulation of DAG in WAT, BAT, testis, skeletal muscle, and cardiac muscle (35). Incubation of WAT from $HSL^{-/-}$ mice with the β-adrenergic agonist isoproterenol resulted in a significant decrease in fatty acid (FA) and glycerol release when compared to WAT from WT mice; however, lipolysis was still observed (35). These data suggest that there are other lipases compensating for HSL's absence, which led investigators to search for additional lipases and led to the discovery of ATGL.

Adipose Triglyceride Lipase.

The identification of the major adipose TAG lipase was made by three research groups that provided 3 different names: adipose triglyceride lipase (ATGL), desnutrin, and calcium independent phospholipase A2ζ (iPLA2ζ) (45–47). ATGL is relatively ubiquitously expressed in humans and mice, however, its expression is highest in WAT and BAT, and lower in skeletal muscle, cardiac muscle, and testis (46–48). During fasting in mice, ATGL mRNA expression increases in adipose tissue, suggesting that ATGL is important in mobilizing fatty acids during stimulated lipolysis (29). ATGL has been shown to hydrolyze TAG, cleaving a fatty acyl chain, when overexpressed in cells and in *in vitro* assays (45–47). The lipase cannot cleave DAG and is therefore known primarily as a TAG lipase (12).

ATGL catalyzes the first step of lipolysis with substrate-specificity. When overexpressed in COS-7 cells, ATGL hydrolyzes only TAG, while DAG accumulates (47). Furthermore, an increase in ATGL expression in differentiated 3T3-L1 adipocytes is followed by an increase in basal release of fatty acids and glycerol (47). These data support ATGL's enzymatic preference for TAG and its role in basal lipolysis. ATGL's hydrolysis of TAG is activated by β-adrenergic stimulation (49,50). *In vivo* studies revealed that ATGL is phosphorylated by PKA, yet the phosphorylation only moderately increases enzymatic activity (51). The same site in ATGL has been identified as a site for phosphorylation by AMPK (52), but given that AMPK is associated with the inhibition of lipolysis, whereas PKA is associated with stimulated lipolysis, this observation has implication. ATGL localizes to both the endoplasmic reticulum and LDs and upon stimulation of lipolysis in cultured adipocytes, ATGL recruitment to LDs is increased

(53,54). PKA-mediated phosphorylation of ATGL may contribute to the control of ATGL activity, subcellular localization, or interaction with co-factors. The phosphorylation controversy has not been resolved and the consequences of phosphorylation of ATGL remain unclear. Additional work is needed to elucidate the mechanism.

To study ATGL's physiological function, the Zechner group developed a mouse model with a genetic deletion of ATGL ($ATGL^{-/-}$ mouse) (49). These mice exhibited mild obesity with increased whole body fat mass, adipocyte hypertrophy, and TAG accumulation in several tissues, mainly heart, testis, and kidneys when compared to WT mice (49). Histological analysis of WAT and BAT showed an accumulation of enlarged LDs, suggesting impaired TAG hydrolysis. Isoproterenol-stimulated WAT explants from $ATGL^{-/-}$ mice exhibited a significant reduction in free FA and glycerol release when compared to WAT from WT mice. These data were supported by findings of reduced TAG hydrolase activity in adipocyte lysates from $ATGL^{-/-}$ mice (49). The most significant phenotype of the ATGL-null mouse was the accumulation of excessive cardiac TAG leading to congestive heart failure and premature death (49). This interesting finding reveals ATGL's imperative function in cardiac energy metabolism. Overall, these studies highlight ATGL's role as a major TAG lipase, however, deletion of ATGL does not result in morbidly obese mice, suggesting that there are other lipases involved in TAG hydrolysis in adipocytes.

Mechanisms by which ATGL activity is regulated are not fully understood. A protein encoded by the G_0/G_1 switch gene 2 (G0S2) binds to and acts as a negative regulator of ATGL (53,55). The knockdown of G0S2 increases the rate of lipolysis, while

overexpression of the protein decreases TAG hydrolysis in cells expressing ATGL (53,55,56). Additionally, ATGL's hydrolase activity is co-activated by Comparative Gene Identification-58 (CGI-58).

CGI-58 and Neutral Lipid Storage Disorder

CGI-58 was discovered through the alignment of the *Caenorhabditis elegans* proteome to predicted amino acid sequences for novel human homologous genes (57). CGI-58 is the 5th member of the α/β hydrolase (ABHD) protein family hence, is sometimes called ABHD5. It is a member of the ABHD subfamily that includes esterases, lipases, and thioesterases (11). Members of this protein family have a conserved catalytic triad that contains a nucleophilic serine residue within the consensus sequence GXSXG, an acidic residue such as aspartate, and a basic residue such as histidine. CGI-58 is unique in that the serine residue of its putative catalytic triad is replaced with an asparagine (11), making it lack lipase activity (12).

In 1974, a rare autosomal disorder called Chanarin-Dorfman syndrome, or Neutral Lipid Storage Disorder (NLSD) was described (58). Patients with NLSD have increased TAG storage in cells that usually do not store much TAG, such as hepatocytes, keratinocytes and neutrophils (58–61). Severe ichthyosis, hepatosteatosis, hearing loss, stunted growth, and mental retardation are symptoms of the disorder, however the patients are not obese. In 2001, researchers identified the cause of NLSD as mutations in CGI-58. Several point mutations, truncations, and frame shifts have been identified in the gene encoding CGI-58 in humans (11,62,63). This phenotype suggests the importance of CGI-58 in TAG turnover in tissues other than adipose, such as skin and liver.

Later, researchers were able to categorize patients with NLSD into two categories: NLSD with ichthyosis (NLSDi) or NLSD with myopathy (NLSDm) (64). Patients with NLSDm suffer from cardiomyopathy and skeletal muscle myopathy, but do not have ichthyosis. This disorder is caused by mutations in both alleles of ATGL resulting in reduced TAG degradation in many tissues, but most importantly heart (64). The connection between NLSDm and loss of ATGL function is supported by cell and animal experiments; the silencing of ATGL in cells and its deletion from mice induces TAG accumulation and cardiomyopathy (49). Interestingly, NLSDm is distinct from NLSDi, which is caused by mutations in the gene encoding CGI-58 and is characterized by ichthyosis and hepatomegaly, but not cardiomyopathy. This indicates the importance of CGI-58 for both TAG turnover and a potentially as yet uncharacterized ATGL-independent function in tissues, particularly skin and liver.

In adipocytes, endogenous PLIN1 mediates the reversible binding of CGI-58 to LDs (26). Under basal conditions, CGI-58 binds to PLIN1 on the surfaces of LDs, and upon stimulation of lipolysis, CGI-58 disperses into the cytoplasm, which is the opposite of what researchers had expected for a factor that is important in TAG turnover (26). It was shown that CGI-58 binds to a 48-amino acid sequence near the carboxyl terminus of PLIN1, but only when cells are incubated under basal conditions (26). The activation of lipolysis promotes the dispersion of CGI-58 into the cytoplasm through phosphorylation-mediated events, which is needed for CGI-58's interaction with ATGL. The PKA-mediated phosphorylation of two serine residues at the carboxyl terminus of PLIN1 (65) and the phosphorylation of CGI-58 are both needed for the efficient release of CGI-58 into the cytosol (Brasaemle and co-workers, unpublished). Similarly, in cells expressing

ectopic PLIN1, CGI-58 co-localizes with PLIN1 on the surfaces of LDs under basal conditions and disperses into the cytosol when lipolysis is stimulated (26). The current model is that the sequestration of CGI-58 by PLIN1 under basal conditions keeps basal lipolysis low, whereas the dispersion of CGI-58 from PLIN1 facilitates CGI-58 binding to and co-activation of ATGL when lipolysis is stimulated.

The Zechner group created a CGI-58 knockout mouse (CGI-$58^{-/-}$) to study the physiological function of CGI-58 (66). Unfortunately, these mice died within the first day of life and were much smaller than newborn WT mice. Analysis of the CGI-$58^{-/-}$ mouse carcass showed significant accumulation of TAG (1.8-fold more than WT mice) (66). The finding of high TAG levels in the carcass indicated that CGI-58 plays an important role in turnover of TAG. The knockout mice had extremely dry and rigid skin that restricted their movement and inhibited them from suckling. Additionally, the mouse carcass turned completely blue when immersed in toluidine blue dye solution, indicating a skin barrier defect and dehydration of the mice (66). These observations were not noted in the $ATGL^{-/-}$ mice, suggesting that CGI-58 has a function independent of ATGL, specifically that CGI-58 is essential for the normal formation of skin, whereas ATGL is not.

In 2005, a novel point mutation in exon 3 of the CGI-58 gene (A245G), which results in a histidine to arginine substitution at amino acid position 82 in humans, was identified (67). This histidine residue is highly conserved across species including mouse, rat, pig, chicken, Japanese quail, and turkey (Figure 1). In this thesis, we studied the consequences of the human H82R mutation in CGI-58 by studying the comparable mouse CGI-58 H84R mutaiton and an H84A mutation.

CGI-58 co-activates ATGL

CGI-58 acts as a co-activator of ATGL's TAG hydrolase activity. *In vitro*, CGI-58 binds to ATGL in a 1:1 molar ratio, increasing ATGL's TAG hydrolase activity by up to 20-fold (12). This functional interaction has been demonstrated when mixing post-nuclear cell extracts containing ectopic CGI-58 with cell lysates expressing ectopic ATGL. Although purifications of both proteins have been reported, most assays showing this synergizing effect have used unpurified ATGL and CGI-58, suggesting that there may be additional factors in the lysates that make a potential contribution to the stimulation of lipolysis. The mechanism by which CGI-58 increases ATGL activity is unknown. CGI-58 alters the regioselectivity of ATGL; in the presence of CGI-58, ATGL cleaves TAG to sn-1,3 and sn-2,3 DAG (68). In the absence of CGI-58, only sn-1,3 DAG is formed (68). The DAG products formed by ATGL in the presence of CGI-58 are not substrates for phospholipid synthesis, rather, can only be used for hydrolysis by HSL or re-esterification by diacylglycerol-O-acyltransferase 2 (DGAT2) (68). It is unclear whether the altered stereochemistry of DAG has an effect on the enzyme activity of ATGL. More work is needed to determine the mechanism by which CGI-58 co-activates ATGL.

It was recently discovered that amino acids 1-254, out of 486 amino acids, are critical for ATGL's lipase activity (69). Truncation of the carboxyl terminus of ATGL yields a protein with increased enzymatic activity *in vitro* that is unable to localize to lipid droplets in cultured cells (69). These data suggest that the C-terminal end of ATGL is inhibitory to TAG hydrolytic activity but needed for the recruitment of ATGL to lipid droplets. One theory is that when bound to ATGL, CGI-58 causes a conformational

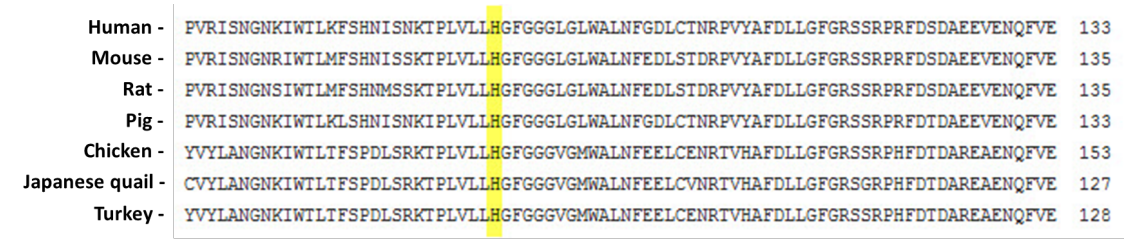

Figure 1. Alignment of CGI-58 amino acid sequences of various species showing the conserved histidine residue

The amino acid sequences of portions of CGI-58 are aligned for human (NP_057090), mouse (NP_080455), rat (NP_997689), pig (NP_001012407), chicken (NP_001265074), Japanese quail (AEL12393), and turkey (AEL12392) using the Basic Local Alignment Search Tool (BLAST).

change in ATGL's structure to move the carboxyl terminus of ATGL and thus relieve the self-inhibition (69). The same research group also examined truncated forms of CGI-58 (70). They reported that truncation of the first 32 amino acids of CGI-58 eliminated CGI-58 binding to ATGL, reduced co-activation of ATGL's TAG lipase activity, and reduced localization of CGI-58 to lipid droplets (70). Collectively, these results suggest that the carboxyl terminal region of ATGL and the amino terminal region of CGI-58 are important to the interaction of these proteins and the consequent co-activation of ATGL.

Multiple theories have been suggested to explain CGI-58's biological activities, including the model in which CGI-58 causes a conformation change in ATGL's structure. Another hypothesis is that CGI-58 is needed as an anchor for ATGL on the surfaces of lipid droplets to bring the lipase to its substrates (70,71). To date, the mechanism of how CGI-58 co-activates ATGL hydrolase activity is unclear. Further research is needed to

determine the exact mechanism by which CGI-58 is able to increase the TAG lipase activity of ATGL. Moreover, data from mouse models and humans suggest that CGI-58 has additional functions independent of the co-activation of ATGL.

Summary of lipolysis

Lipid droplets are dynamic organelles that store TAG and are the site of lipid mobilization. Intracellular lipid metabolism requires multiple proteins that are key regulators of lipolysis (Figure 2). Three lipases are needed for the full hydrolysis of TAG: ATGL, HSL, and MGL. Other proteins serve regulatory functions, including PLIN1, CGI-58, and G0S2.

In the basal state, PLIN1 sequesters CGI-58 on the surface of lipid droplets making CGI-58 unable to interact with and co-activate ATGL (26,65). ATGL is localized on both the surfaces of LDs and in the cytoplasm under basal conditions. Furthermore, binding of G0S2 to ATGL results in the inhibition of TAG hydrolysis (53,55,56). Hormone sensitive lipase is also inactive and localized in the cytosol (23,42). These conditions collectively reduce lipolysis and promote TAG storage.

In times of energy deprivation, starvation, and endurance exercise, or stimulated conditions, lipolysis is stimulated by a variety of hormones, including catecholamines. Several proteins are then phosphorylated by PKA, including HSL, PLIN1, CGI-58 (Brasaemle and co-workers, unpublished), and likely ATGL (13,41,51). Upon phosphorylation, HSL translocates to the surfaces of lipid droplets where it docks in a protein-protein interaction with phosphorylated PLIN1 (23,24). The phosphorylation of PLIN1 and CGI-58 results in the release of CGI-58, which then binds with ATGL to the surfaces of lipid droplets (26,65,71). Once the lipases have gained access to their

substrates, ATGL hydrolyzes TAG with the help of CGI-58, and HSL catalyzes the conversion of DAG into MAG by cleaving off another fatty acyl chain. The remaining MAG is hydrolyzed by MGL to remove the final fatty acid (72). Fatty acids and glycerol are released into circulation and are delivered to other tissues. Experimentally, we are able to induce this lipolytic pathway by incubating cells with forskolin, an activator of adenylyl cyclase, and isobutylmethylxanthine (IBMX), a phosphodiesterase inhibitor.

It is important to note that not all cells express PLIN1, and that the other perilipins function to control lipolysis in different ways. The control of lipolysis is dependent upon which perilipins are expressed within a given tissue. PLIN2 is ubiquitously expressed in mouse tissues (73), however, since it is unable to sequester CGI-58, PLIN2 is not protective against ATGL-mediated TAG hydrolysis (71). LDs in cells and tissues where triacylglycerols accumulate in NLSD patients, such as hepatocytes, skin cells and white blood cells, are coated with PLIN2. PLIN3 is also ubiquitously expressed, but is associated with LD formation, rather than control of lipolysis at the surfaces of mature lipid droplets (22). Notably, PLIN5 is highly expressed in heart, skeletal muscle, and brown adipose tissue. PLIN5 is able to bind CGI-58 and ATGL individually, but the mechanism by which it regulates lipolysis needs to be elucidated (71).

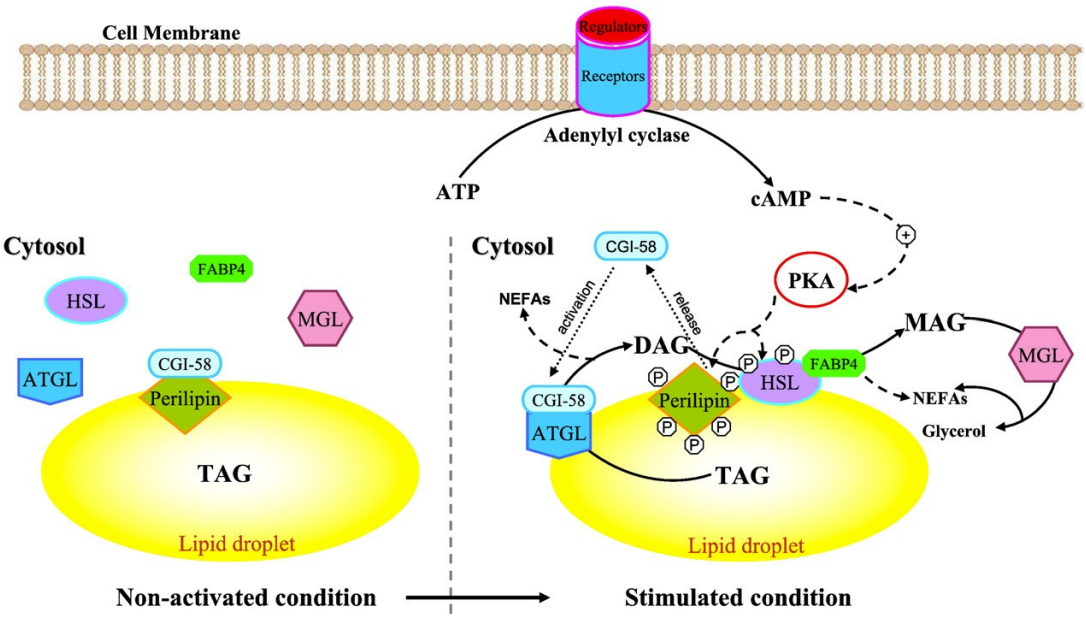

Figure 2. Regulation of lipolysis in adipocytes.

Under basal conditions, PLIN1 sequesters CGI-58 on the surfaces of lipid droplets preventing it from co-activating ATGL. ATGL is localized to both the cytosol and lipid droplets while HSL remains in the cytosol. Upon stimulation of lipolysis, an increase in cAMP leads to the phosphorylation of PLIN1 and HSL by PKA. CGI-58 is consequently released from PLIN1 and binds with ATGL to the surfaces of lipid droplets to hydrolyze TAG. HSL relocates to the surfaces of lipid droplets where it interacts with PLIN1 and hydrolyzes DAG. The subsequent MAG is cleaved by MGL. Figure reproduced from Lampidonis *et al*., 2011 with permission from Elsevier (74).

Specific Aims

CGI-58 plays an important role in lipid homeostasis by acting as a co-activator of ATGL. However, the mechanism by which it does so is still unclear and more research is needed to address it. To elucidate mechanisms for protein function, researchers often study naturally occurring mutations that alter protein function. This project aims to characterize the naturally occurring mutation in CGI-58, H82R, which causes NLSDi in humans; the corresponding mutation in mouse CGI-58 is H84R. We hope to gain understanding of the mechanism by which CGI-58 activates ATGL hydrolase activity. We also studied mouse CGI-58 with a H84A mutation to better understand the importance of the histidine residue at position 84. Because the H82R mutation in CGI-58 causes NLSDi in humans, we hypothesized that histidine 84 is a critical residue in the function, localization, and binding of mouse CGI-58 to either ATGL or lipid substrates. The hypothesis was tested in the following aims:

Aim 1: To investigate the activity of CGI-58 with mutations of H84A and H84R in activation of ATGL. We tested whether the H84A and H84R mutations in mouse CGI-58 could synergize ATGL's TAG hydrolase activity *in vitro*. We also tested whether ectopically expressed, CGI-58 with either the H84A or H84R mutations would be efficient at reducing excess TAG levels of NLSDi cells when compared to WT CGI-58.

Aim 2: To determine the subcellular localization of CGI-58 with mutations H84A and H84R in PLIN1-expressing cells. We studied whether H84A or H84R mutations would alter the binding of CGI-58 to PLIN1 on the surfaces of lipid droplets under basal conditions or alter CGI-58 release into the cytosol under stimulated conditions.

Aim 3: To analyze the binding of CGI-58 with H84A or H84R mutations to ATGL and the recruitment of the complex to lipid droplets. We tested whether the mutations would alter CGI-58 binding to ATGL or the ability of the protein complex to gain access to its lipid substrates in lipid droplets.

MATERIALS

Dulbecco's Modified Eagle Medium (DMEM), glycine, and ScintiVerse BD Cocktail were purchased from Fisher Scientific, Inc (Waltham, MA). Minimum Essential Medium (MEM), Clean-Blot IP Detection Reagent HRP used as a secondary antibody, Infinity™ Triglycerides Liquid Stable Reagent, and Beckman Centrifuge Tubes (polyallomer 14 x 89 mm) were purchased from Thermo Fisher Scientific, Inc. (Middletown, VA). Bovine calf serum was purchased from Gemini Bio-Products (West Sacramento, CA). Geneticin (G418) was purchased from Gold Biotechnology, Inc (St. Louis, MO). Penicillin/streptomycin and Protein A Sepharose beads were purchased from Life Technologies (Carlsbad, CA). Fetal bovine serum, oleic acid, forskolin, 3-isobutyl-1-methylxanthine (IBMX), dimethyl sulfoxide (DMSO), cesium chloride (CsCl), ethanolamine, triethanolamine, dimethyl pimelimidate dihydrochloride (DMP), Isopropanol, hexane, di-ethyl ether, and saponin were purchased from Sigma-Aldrich, Co. (St. Louis, MO). Fatty acid-free bovine serum albumin (FAF BSA) was purchased from US Biological (Swampscott, MA). Protease inhibitor cocktail pills were purchased from Roche Diagnostics (Indianopolis, IN). *DC* Protein Assay reagents were purchased from Bio-Rad Laboratories, Inc. (Hercules, CA). TALON® Metal Affinity Resin was purchased from Clontech Laboratories, Inc. (Mountain View, CA). Solution of 4% paraformaldehyde in PBS was purchased from Affymetrix, Inc. (Cleveland, OH). SlowFade® Anti-Fade kit was purchased from Molecular Probes, distributed by Invitrogen (Eugene, OR). Radiolabeled [^{3}H] triolein was purchased from PerkinElmer Life Sciences (Boston, MA). Hydrofluor was purchased from National Diagnostics (Altanta, GA).

Polyclonal anti-CGI-58 serum was reported previously (26). Rabbit polyclonal antibody raised against ATGL was purchased from Cell Signaling Technology, Inc. (Danvers, MA; product #2138). Peroxidase-conjugated goat anti-rabbit antibodies were purchased from Sigma-Aldrich, Co. (St. Louis, MO). Anti-goat Alexa Fluor 546, and anti-rabbit Alexa Fluor 488 were purchased from Molecular Probes, distributed by Invitrogen (Eugene, OR). Amersham™ Enhanced Chemiluminescence Western Blotting Analysis System was purchased from GE Healthcare (UK). SuperSignal West Femto Chemiluminescent Substrate was purchased from Thermo Fisher Scientific, Inc. (Middletown, VA).

Human NLSDi cells were generously donated by Dr. Rosalind A. Coleman (University of North Carolina – Chapel Hill). Goat polyclonal anti-perilipin antiserum was the generous gift of Dr. Constantine Londos (National Institutes of Health, Bethesda, MD). Dr. Derek McMahon generously provided all of the unpurified CGI-58 adenoviruses and the BL21 *E. coli* cells containing cDNA for CGI-58, including WT and H84A and H84R mutated CGI-58. Mrs. Mayda Hernandez kindly provided the purified ATGL adenovirus.

METHODS

Mammalian Cell Culture

AD293 human embryonic kidney cells were used for the amplification of adenoviruses and to provide lipid droplets for the lipid droplet binding assay. These cells were cultured in DMEM supplemented with 10% fetal bovine serum, 100 units/ml penicillin, and 100 μg/ml streptomycin at 37°C in a humidified incubator with a 5% CO_2 atmosphere.

For immunoprecipitations and to express proteins for lipid droplet binding assays, COS-7 African green monkey kidney cells were cultured in DMEM supplemented with 10% fetal bovine serum, 100 units/ml penicillin, and 100 μg/ml streptomycin at 37°C in a humidified incubator with a 5% CO_2 atmosphere.

NIH 3T3 CARΔ fibroblasts were used for CGI-58 and PLIN1 co-localization experiments. NIH 3T3 mouse fibroblasts were engineered to express a truncated version of the coxsackie and adenovirus receptor (CARΔ) that encodes a cell surface receptor lacking a cytoplasmic signaling domain (75). The expression of CARΔ enhances adenovirus uptake, leading to increased expression of ectopic proteins. These cells were cultured in DMEM supplemented with 10% bovine calf serum, 100 units/ml penicillin, 100 μg/ml streptomycin, and 800 μg/ml G418 antibiotic to maintain expression of CARΔ, and were grown at 37°C in a humidified incubator with a 5% CO_2 atmosphere.

NLSDi human skin fibroblasts were used to determine the effect of CGI-58 mutations on CGI-58 function in triacylglycerol turnover. They were cultured in MEM supplemented with 1% non-essential amino acids, 10 mM sodium pyruvate, 10% fetal

bovine serum, 100 units/ml penicillin, and 100 μg/ml streptomycin and were grown at 37°C in a humidified incubator with a 5% CO_2 atmosphere.

Adenovirus Amplification & Purification

CGI-58 wild-type (WT), H84A, and H84R adenoviruses were amplified in AD293 cells; 3.5 x 10^6 cells were seeded in 145 mm dishes. The cells were transduced with dilutions of unpurified adenoviruses to produce a high titer amplification within 3-5 days. Infected AD293 cells were harvested, and lysed, and the adenovirus was purified by cesium chloride (CsCl) ultracentrifugation (76).

Adenoviral Transductions

NIH 3T3 CARΔ fibroblasts or COS-7 cells were seeded into dishes as indicated for specific experiments 24 hours before transduction. Adenovirus was added to the media and cells were incubated with the adenovirus media for 24 hours at 37°C in 5% CO_2. After 24 hours, media containing the adenovirus was replaced with growth media and cells were incubated for another 24 hours. Forty-eight hours after transduction, cells were harvested and re-suspended in lysis buffer. Uninfected cells and cells transduced with adenovirus to drive the expression of β-galactosidase were used as negative controls.

Purification of Recombinant CGI-58

BL21 *E. coli* containing cDNA for 12-His-tagged CGI-58 with point mutations H84R and H84A and WT CGI-58 in the pET-28a vector were grown in Luria Broth (LB) supplemented with kanamycin for 16 hours while shaking at 37°C. Cells were transferred to larger volumes of LB and grown to an optical density of 0.5-0.8 at a wavelength of 595 nm. Isopropyl β-D-1-thiogalactopyranoside (IPTG) (1 mM) was added to induce the expression of T7 RNA polymerase, and consequently, CGI-58. Cells were incubated

while shaking at 37°C for 3-5 hours, and then harvested, centrifuged at 4,000 x g for 10 minutes at 4°C, and stored at -20°C until ready for use.

Frozen cell pellets were thawed and re-suspended in a lysis buffer containing 50 mM Tris, pH 7.5, 100 mM KCl, 1 mM DTT, 30 mM imidazole, 10% glycerol, 1 mg/ml lysozyme, 1 EDTA-free protease inhibitor cocktail tablet, and 0.01% Ige Pal (only for mutated variants of CGI-58). After 30-minute incubation on ice, cells were disrupted using a Bead Beater for 15 cycles of 10 seconds separated by 50 second cooling intervals. The cell lysate was then centrifuged at 21,000 x g at 4°C for 20 minutes and the supernatant was incubated with TALON® Metal Affinity Resin, for His-Tag purification, while rotating end-over-end overnight at 4°C. The mixture was centrifuged at 4°C and the resin was re-suspended in wash buffer composed of lysis buffer with 100 mM imidazole. The re-suspended resin in wash buffer was poured into a small column. The 12-His-tagged CGI-58 was eluted with 9 ml of elution buffer (composed of lysis buffer with 250 mM imidazole and 40% glycerol). Eluted proteins were stored at -20°C until further use.

Co-immunoprecipitations

To assess the binding of CGI-58 to ATGL, COS-7 cells were seeded in 100 mm dishes at a density of 1 x 10^6 cells 24 hours before one of each of the CGI-58 variant and ATGL adenoviruses were simultaneously transduced into the same cells. For one experiment, cells were lipid-loaded with 400 μM oleic acid complexed to fatty acid free bovine serum albumin (FAF BSA) (4:1 molar ratio) for 16 hours prior to harvest and lipolysis was stimulated 30 minutes before harvest by adding 10 μM forskolin and 0.5 mM isopropyl β-D-1-thiogalactopyranoside (IBMX) diluted in 2.5% FAF BSA –

DMEM. Forty-eight hours post-transduction, media were removed, and cells were rinsed with phosphate buffered saline (PBS), harvested, and re-suspended in 1 ml of non-denaturing lysis buffer containing 50 mM Tris HCl, pH 7.4, 150 mM NaCl, 1% NP-40, 1 mM EDTA, 10 mM NaFl, and 1x protease inhibitor cocktail. Samples were incubated on ice for 15-30 minutes and pulled through a 23-gauge needle multiple times to complete disruption of cells. Protein concentrations of samples were determined using the *DC* protein assay. Lysate volumes containing 800 µg of total protein were used for the immunoprecipitations and 30 µg was reserved for immunoblotting. Samples were pre-cleared by incubating with 20 µl Protein A-Sepharose beads at 4°C for 1 hour while mixing by turning end-over-end.

For each sample, 60 µl of Protein A-Sepharose beads (120 µl slurry) were washed with 1 ml PBS followed by 1 ml wash buffer containing 50 mM Tris HCl, pH 7.4, 150 mM NaCl, 1% NP-40, 1 mM EDTA, and 10 mM NaF before sample addition. Either 10 µg/ml rabbit IgG (negative control) or 7 µl CGI-58 antiserum was added to the Protein A-Sepharose beads and incubated with end-over-end mixing overnight at 4°C. The antibodies were cross-linked to the beads by washing the beads with 200 mM triethanolamine, pH 8.9, then incubating with 50 mM dimethyl pimelimidate dihydrochloride (DMP) in 200 mM triethanolamine for 4 hours at 4°C followed by 1 hour at room temperature while mixing. The beads were washed with 200 mM triethanolamine and then incubated with 100 mM ethanolamine for 30 minutes at room temperature.

The pre-cleared sample was then added to the cross-linked beads and incubated with end-over-end mixing for 3 hours at 4°C. After the incubation, the beads were

washed 5 times using the wash buffer. To elute the proteins off of the beads, 60 µl of 2x Laemmli sample buffer (LSB) was added and the samples were boiled for 10 minutes (77). The supernatant was collected and stored at -20°C until further use.

Immunofluorescence Microscopy

Subcellular localization of PLIN1 and CGI-58 under basal and lipolytically stimulated conditions was determined using NIH 3T3 CARΔ cells that were seeded in 60 mm dishes at a density of 3 x 10^5 cells 24 hours prior to simultaneous transduction with CGI-58 variant and PLIN1 adenoviruses. At 24 hours after transduction, cells were transferred onto glass coverslips in 6-well dishes. At 36 hours, cells were lipid loaded with 200 µM oleic acid complexed to FAF BSA (4:1 molar ratio) for 12 hours. For stimulation of lipolysis, media containing 10 mM forskolin and 0.5 mM IBMX with 2% FAF BSA were added to the cells and cells were incubated for 30 minutes at 37°C. For basal conditions, cells were incubated with fresh DMEM containing 2% FAF BSA for 30 minutes. All cells were rinsed with PBS and fixed in 4% paraformaldehyde in PBS for 20 minutes at room temperature. After several washes with PBS, the cells were incubated in a solution containing 0.2 M glycine (to quench reactive aldehydes), 0.1 mg/ml saponin (to permeabilize cells), and 0.2 mg/ml rat IgG (to block non-specific binding sites) in PBS for 1 hour at room temperature. Coverslips were then transferred to 24-well dishes where they were washed with PBS and incubated with goat anti-perilipin (1:5,000) and rabbit anti-CGI-58 (1:5,000) antisera diluted in PBS with 0.1 mg/ml saponin and 0.2 mg/ml rat IgG for 1 hour at room temperature. Cells were washed in PBS and incubated for 1 hour at room temperature with anti-goat Alexa Fluor 546 (1:5,000) and anti-rabbit Alexa Fluor 488 (1:5,000). Stained cells were washed in PBS and mounted onto glass

slides using reagent A from the SlowFade® Anti-fade kit and sealed with clear nail polish. Cells were viewed using a Nikon Eclipse E800 fluorescence microscope and images were captured using a Photometrics CoolSNAP *EZ* digital camera. NIS Elements software was used to process the images. Two individuals blinded to sample identity performed cell counts. A minimum of 100 cells were counted for each condition and cells were scored for either a staining pattern representing CGI-58 co-localized with PLIN1 on lipid droplets or a diffuse pattern of CGI-58 staining in the cytoplasm representing CGI-58 dispersed from PLIN1 and off of the lipid droplets.

Triacylglycerol content of NLSDi cells

NLSDi cells were seeded into 60 mm dishes at a density of 6 x 10^5 and transduced with CGI-58 variant or β-galactosidase adenoviruses. After transduction, NLSDi cells were harvested by trypsinization at 6, 12, 24, and 48 hours. Cells were collected by centrifugation at 1,000 x g for 10 minutes at 4°C. Cell pellets were stored at -80°C until ready for use. To extract lipids, cell pellets were incubated in 2 ml of isopropanol-hexane-water (80:20:2) for 30 minutes at room temperature followed by the addition of 500 µl of hexane-diethyl ether (1:1), mixing, and incubation for 10 minutes (78). To separate the phases, 1 ml of deionized water was added and samples were incubated for 20 minutes at room temperature. A set volume (600-800 µl) of the organic phase (top layer) was collected and evaporated using a Speed Vac Concentrator equipped with a cold trap. The dried lipids were then incubated with 300 µl of Infinity™ Triglycerides Stable Reagent for 1-2 hours with shaking at 37°C. After incubation, samples were transferred to a 96-well plastic microplate and the absorbance of samples was measured

at 540 nm. Corn oil provided a source of TAG for standards. Various amounts of corn oil were extracted and analyzed using the same methods to develop a standard curve.

Lipid Droplet Binding Assay

This protocol was generously shared with us by Dr. Laura Listenberger (St. Olaf College, Northfield, MN). In this assay, CGI-58 and ATGL were incubated with lipid droplets to assess the recruitment of proteins to lipid droplets. Lipid loaded AD293 cells were the source of lipid droplets for this experiment. AD293 cells were seeded in 145 mm dishes and, after 36 hours, were lipid loaded with 1 mM oleic acid complexed to FAF BSA (4:1 molar ratio) overnight at 37°C. Cells were harvested, centrifuged at 1,000 x g for 10 min at 4°C to pellet cells, then resuspended in 1.5 ml hypotonic lysis buffer containing 10 mM NaF, 1 mM EDTA, and 1x protease inhibitor cocktail in 20 mM Tris, pH 7.4. Cells were incubated on ice for 10 minutes before a cold glass homogenizer with Teflon pestle was used to shear the cells with 10 strokes. Cell homogenates were stored on ice until further use.

For a source of ATGL and CGI-58, COS-7 cells were seeded in 100 mm dishes at a density of 1 x 10^6 and, 24 hours later cells were transduced with purified adenoviruses for the expression of ATGL and one of each of the CGI-58 variants in the same cells. Forty-eight hours after transduction, cells were harvested, centrifuged at 1,000 x g for 10 minutes at 4°C, then re-suspended in 900 µl hypotonic lysis buffer, incubated on ice for 10 min, and sheared using a homogenizer, as described above. Samples were then centrifuged for 30 minutes at 15,000 x g at 4°C to remove unbroken cells, nuclei, and heavy membranes. A small volume of sample was reserved for immunoblotting.

Protein and lipid droplet samples were mixed and incubated while rotating end-over-end for 1 hour at room temperature. A volume of cold 60% sucrose in hypotonic lysis buffer was added to the mixture to give a final concentration of 20% sucrose. Samples were added to centrifuge tubes (Beckman polyallomer 14 x 89 mm) and then overlaid with 5 ml of cold 5% sucrose in hypotonic lysis buffer, followed by 5 ml of hypotonic lysis buffer. The gradient-filled tubes were centrifuged at 27,000 x g in a SW41Ti rotor for 30 minutes at 4°C. No brake was applied; the rotor was allowed to coast to a stop. After centrifugation, the floating lipid droplet layer (top layer) was collected in a minimal volume using a Beckman tube slicer. SDS was added to the samples for a final concentration of 5%. To solubilize lipid droplet-associated proteins, samples were incubated with sonication at 60°C in a Branson 8510 heated water bath sonicator for 1-3 hours. Samples were then prepared for sodium dodecyl sulfate polyacrylamide gel electrophoresis (SDS-PAGE) and immunoblotting for CGI-58 and ATGL.

TAG Hydrolase Assay

An *in vitro* assay was used to evaluate the ability of H84R and H84A CGI-58 to co-activate the TAG hydrolase activity of ATGL. Volumes corresponding to 50 µg of protein from COS-7 cell lysates of cells ectopically expressing ATGL and 1 µg of partially purified recombinant CGI-58 (or CGI-58 variants) were mixed in 0.1 M potassium phosphate buffer, pH 7.0. A volume of 100 µl of substrate containing 330 µM [9,10-^{3}H] triolein emulsified with 145 µM phosphatidylcholine:phosphatidylinositol (PC:PI) (3:1) was added to the mixture (79). The mixtures were incubated for 1 hour at 37°C and reactions were terminated by adding 3.25 ml of methanol:chloroform:heptane

(10:9:7), 1.05 ml of 0.1 M potassium carbonate and 0.1 M boric acid, pH 10.5. Samples were centrifuged at 800 x g for 20 minutes at room temperature followed by the removal of 1 ml from the top phase that was then added to 10 ml of Hydrofluor Scintillant. Quantification of radioactivity was done using a Beckman scintillation counter.

Immunoblot Analysis

For all experiments, samples (total volume) and the cell lysate volumes corresponding to 30 μg of total protein representing the input lysate, were boiled for 5 minutes to solubilize and denature the proteins. Proteins were then separated by SDS-PAGE and then electrophoretically transferred to nitrocellulose membranes for immunoblot analysis. The membrane was blocked in 5% non-fat milk diluted in TBST containing 20 mM Tris, pH 7.6, 150 mM NaCl, 0.02% Tween-20, and then incubated with CGI-58 antiserum (1:25,000) and ATGL antibody (1:1,000) diluted in 5% BSA in TBST. For detection of primary antibodies, Clean-Blot IP Detection Reagent HRP (1:10,000) was used for immunoprecipitation experiments and peroxidase-conjugated goat anti-rabbit antibody (1:5,000) was used for all other experiments. Proteins were detected using either SuperSignal West Femto reagent followed by X-ray film exposure or Enhanced Chemiluminescence Reagent followed by FluorChem M digital darkroom exposure.

Statistical Analysis

Data were analyzed using GrahPad Prism 6 software. Data represent the means of duplicate or triplicate samples ± either the standard deviation or standard error of the mean. Variance was measured using ANOVA.

RESULTS

H84R CGI-58 does not reduce excess TAG levels in NLSDi human skin fibroblasts

NLSDi cells are a human skin fibroblasts derived from an NLSDi patient. The cultured NLSDi cells that were used in our experiments normally accumulate high levels of TAG due to a mutation in the gene for CGI-58 that results in a truncation of the peptide sequence at amino acid 190 (10,12). Ectopic overexpression of WT CGI-58 in these cells significantly reduces TAG levels (12). It was previously shown by Dr. Derek McMahon and Dharika Shah that expression of the H84R CGI-58 variant results in TAG retention in these cells, yet overexpression of the H84A CGI-58 variant significantly reduced levels of TAG, although not quite to the level of cells expressing WT CGI-58. However, the TAG from this experiment was only analyzed at 48 hours post-transduction of the CGI-58 variant adenovirses. We hypothesized that a more detailed time course would reveal more useful information; the H84A variant might exhibit impaired TAG turnover well before 48 hours, while the H84R variant would likely be consistently inefficient at reducing TAG levels over 48 hours. Thus, we evaluated TAG turnover in a more detailed time course to elucidate differences between the variants.

Before beginning experiments to study the effects of CGI-58 variants in reducing excess TAG in cultured NLSDi cells, it was necessary to define the adenoviral titers needed to drive comparable levels of protein expression for all variants. Having comparable levels of ectopically expressed CGI-58 is important to make sure that the results of the experiment are not due to variations in protein levels of CGI-58. Thus, to normalize the expression of CGI-58 variants, various titers of cesium chloride-purified adenoviruses for WT, H84A, and H84R CGI-58 were tested. Cells were harvested 48

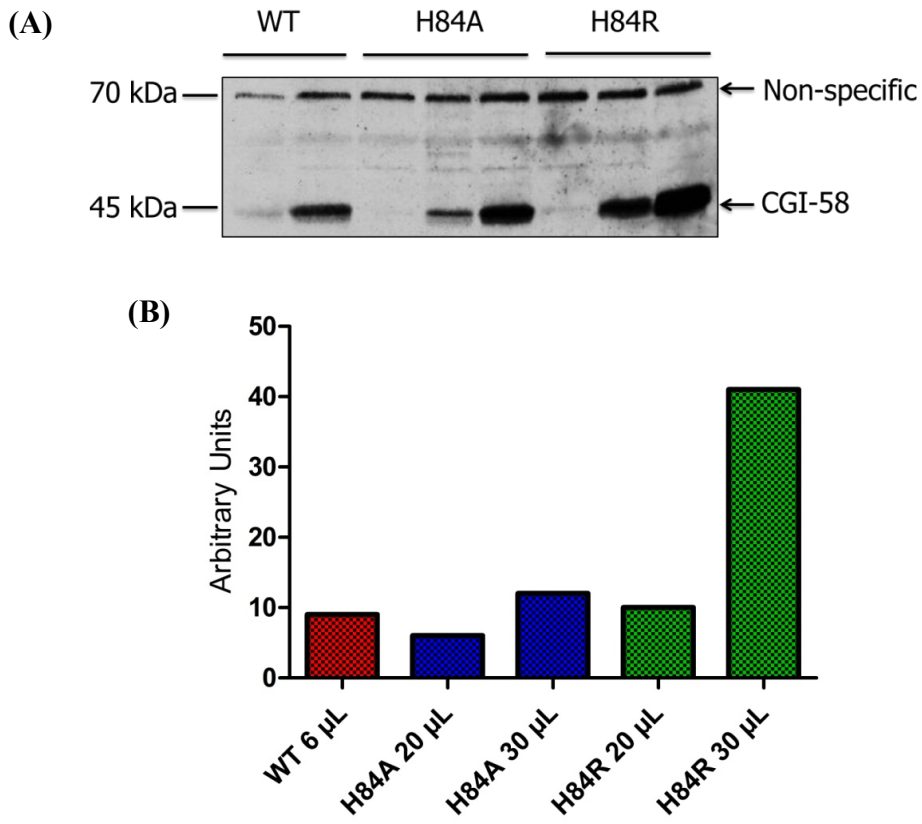

Figure 3. Titration of adenoviral doses for expression of CGI-58 variants in NLSDi human skin fibroblasts

(A) NLSDi fibroblasts were transduced with different titers of adenoviruses for the expression of WT CGI-58 and CGI-58 with H84A and H84R mutations. Cells were harvested 48 hours after transduction and prepared for SDS-PAGE and immunoblotting for CGI-58. The band at 70 kDa is a non-specific band that was used as a control for protein load. (B) Densitometry was performed to analyze each band's density and, with corrections for protein load, viral titers that yielded comparable levels of protein expression for each CGI-58 variant were determined. Data shown correspond to the samples with significant CGI-58 expression in A.

hours post-transduction and lysates were prepared for immunoblotting with rabbit antiserum raised against CGI-58 (Figure 3A). Densitometry was used to quantify the expression of the CGI-58 variants relative to a nonspecific protein band detected by the antiserum that provided a measure of protein loading (Figure 3B). Viral titers that yielded comparable levels of protein expression for each CGI-58 variant were chosen for use in subsequent experiments. For NLSD experiments, 6.5 μl of WT CGI-58, 25 μl of H84A CGI-58, and 20 μl of H84R CGI-58 adenoviruses were selected for transduction of NLSDi cells to yield comparable protein levels of CGI-58. Cells were collected at 6, 12, 24, and 48 hours after transduction for the analysis of cellular TAG levels (Figure 4). Importantly, a viral titer test was performed prior to each subsequent cell experiment so that comparable protein levels were studied. Appropriate viral titers were also determined experimentally for doubly transduced cells when two proteins were expressed in cells.

NLSDi cells accumulate high levels of TAG as shown in uninfected cells harvested before transduction (Figure 4A). Cells transduced with β-galactosidase (negative control) harvested at 48 hours post-transduction accumulated 1.32 μg TAG/μg protein (data not shown), suggesting that the addition of viral vectors does not alter TAG turnover in NLSDi cells. Ectopic overexpression of WT CGI-58 causes reduction of TAG levels starting at 6 hours and continuing to 48 hours. Ectopic H84R CGI-58 was ineffective at reducing TAG levels from 6 hours through 48 hours post-transduction. To our surprise, ectopic expression of H84A mutated CGI-58 shows an almost identical pattern of TAG turnover to WT CGI-58, suggesting that H84A CGI-58 is just as effective as WT CGI-58 at reducing excess TAG levels in NLSDi cells. Importantly, WT CGI-58 and CGI-58 mutations H84A and H84R were expressed at approximately comparable

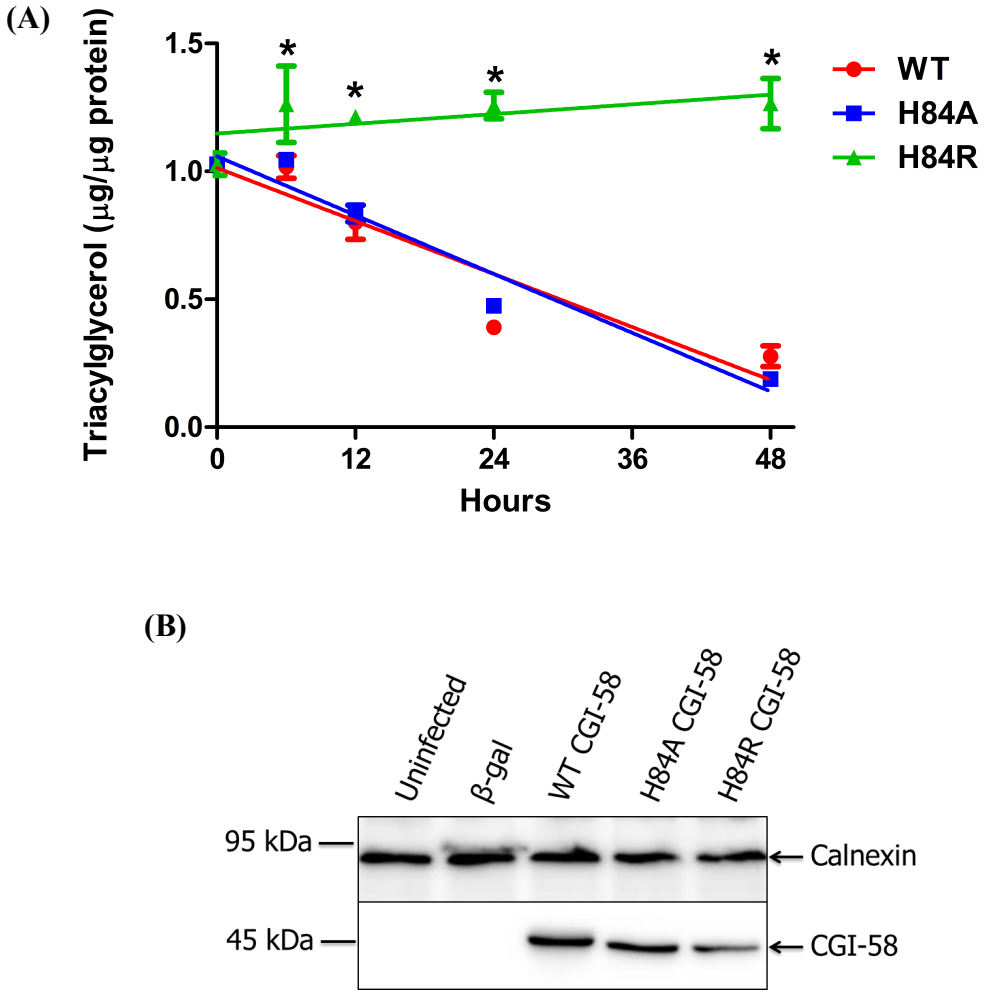

Figure 4. CGI-58 with the H84R mutation is not effective at reducing excessive TAG storage in NLSDi human skin fibroblasts.

(A) NLSDi fibroblasts were transduced with adenovirus for the expression of mutated or WT variants of CGI-58 and then harvested 6, 12, 24, and 48 hours post-infection. Uninfected cells were harvested at 0 hours. TAG content of cells was determined for each time point. Linear regression was used to analyze the data. Data points are the means ± standard error of the mean for triplicate samples. Data are from one representative experiment of three. Where error bars are not visible, they are contained within the symbols. Data were analyzed using two-way repeated measures ANOVA with

Bonferroni *post hoc* test. Data points marked with a star are statistically different from WT and H84A CGI-58 ($p < 0.05$). (B) Cell lysate volumes corresponding to 30 μg of total protein were eluted on an SDS-PAGE gel, transferred to a nitrocellulose membrane, and probed with antiserum raised against mouse CGI-58, β-galactosidase antiserum, and calnexin antibodies. Uninfected cells and cells expressing β-galactosidase lack detectable CGI-58. Cells transduced with β-galactosidase adenovirus (negative control) express β-galactosidase as depicted by the faint band located directly above the calnexin band in B. Cells transduced with CGI-58 variant adenoviruses express comparable protein levels of CGI-58.

levels in cultured NLSDi human skin fibroblasts. Thus, neither mutation destabilizes the protein leading to degradation. These results suggest that H84R CGI-58 lacks the ability to increase TAG turnover, presumably due to its inability to co-activate ATGL's TAG hydrolase activity. However, since an alanine substitution for histidine does not significantly impair TAG turnover, the histidine residue may not be essential for CGI-58 function, but rather the arginine in this position may inactivate the protein. We examined the effects of these mutations on CGI-58 function further.

H84R CGI-58 fails to co-activate ATGL TAG hydrolase activity *in vitro*

To test the hypothesis that the H84R mutation in CGI-58 affects CGI-58's ability to co-activate ATGL, we measured free fatty acid release from TAG in the presence of cell lysates with ATGL and purified recombinant variants of CGI-58. COS-7 cell extracts with ectopic ATGL and 1 μg of recombinant CGI-58 partially purified from *E coli* were mixed with radiolabeled TAG emulsified with PC and PI. Mixtures containing only ATGL exhibited very low TAG hydrolase activity (Figure 5). The addition of WT CGI-58 significantly increased TAG hydrolase activity by 5-fold. In contrast, mutated variant H84R CGI-58 completely failed to co-activate ATGL TAG hydrolase activity. The addition of H84A CGI-58 increased TAG hydrolase activity by approximately 2-fold, but this difference was not statistically different from samples containing only ATGL when the data were analyzed by ANOVA with Tukey's *post hoc* test. However, when the data were analyzed using Student's *t*-test, the activation of ATGL activity by H84A CGI-58 was statistically different from ATGL ($p=.014$), WT CGI-58 ($p=0.032$), and H84R CGI-58 ($p=.009$). It is likely that H84A CGI-58 has some residual activity in increasing TAG

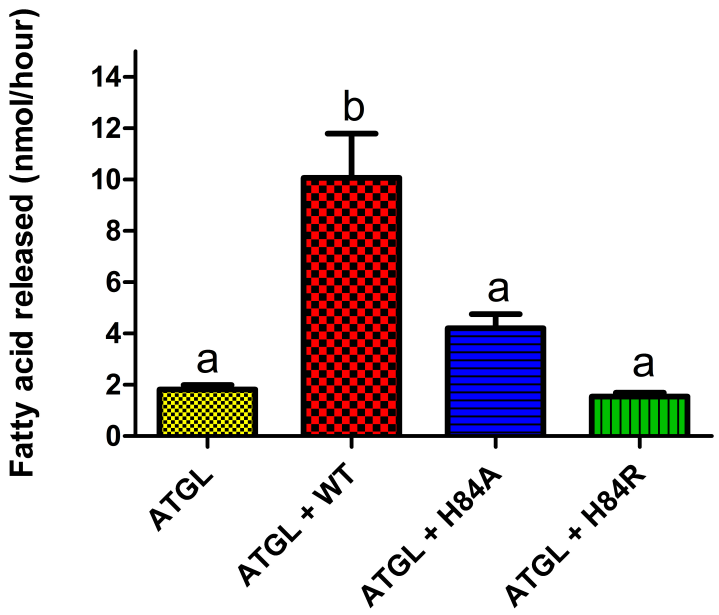

Figure 5. CGI-58 with an H84R mutation does not activate ATGL hydrolase activity *in vitro*

COS-7 cell extracts expressing ATGL (50 µg total protein) were mixed with 1 µg of CGI-58 partially purified from Bl21 *E coli*. Reactions were mixed with [9,10-^{3}H] triolein emulsified with PC:PI (3:1) and incubated for 1 hour at 37°C. Fatty acids were solvent-extracted and quantified by β-scintillation counting. The addition of recombinant WT CGI-58 increased the TAG hydrolytic activity of ATGL. Reactions containing H84A CGI-58 and ATGL display significantly greater TAG hydrolytic activity than that of reactions containing ATGL alone, yet less activity than reactions containing WT CGI-58 and ATGL. The addition of recombinant H84R CGI-58 did not increase ATGL's TAG hydrolytic activity. Data are the mean ± standard deviation of averaged duplicate samples from triplicate experiments. Data were analyzed using by ANOVA with Tukey's *post hoc* test. Samples with different subscripts (a,b) are statistically different from each other ($p < 0.05$).

hydrolysis, since it is comparable to WT in reducing the excessive TAG stores of NLSD cells (Figure 4). These data led us to hypothesize that the histidine to arginine mutation may cause a conformational change in CGI-58 leading to a misfolded protein, which could alter subcellular localization.

Subcellular localization of CGI-58 in PLIN1-expressing cells

Previous studies have shown that CGI-58 localizes to LDs through a binding interaction with PLIN1 under basal conditions, and disperses into the cytoplasm following the stimulation of lipolysis (26). We tested the subcellular localization of the mutated variants of CGI-58 in mouse fibroblasts ectopically expressing PLIN1 (Figures 6A and B). Under basal conditions, PLIN1 and WT CGI-58 co-localized on the surfaces of LDs. The same observations were made with the H84A and H84R CGI-58 variants, suggesting that neither mutation affects CGI-58 binding to PLIN1 under basal conditions (Figures 6A and B). These observations also suggest that neither H84A nor H84R mutations disrupt CGI-58 structure enough to impede CGI-58 binding to PLIN1. Upon stimulation of lipolysis, WT CGI-58 and CGI-58 with mutations H84A and H84R were released from the PLIN1 scaffold into the cytoplasm (Figures 6A and B). Thus, neither the H84A nor the H84R mutation altered the normal PKA-mediated dispersion of CGI-58 into the cytosol. We quantified the subcellular localization of CGI-58 under both basal and stimulated conditions with cell counts of stained cells performed by two individuals blinded to sample identity (Figure 6B). Results of immunoblots show that all variants of CGI-58 were expressed at approximately comparable levels (Figure 6C). Since the mutation does not affect the subcellular localization of CGI-58, we hypothesized that the H84R variant fails to co-activate ATGL because it cannot bind to ATGL.

(A)

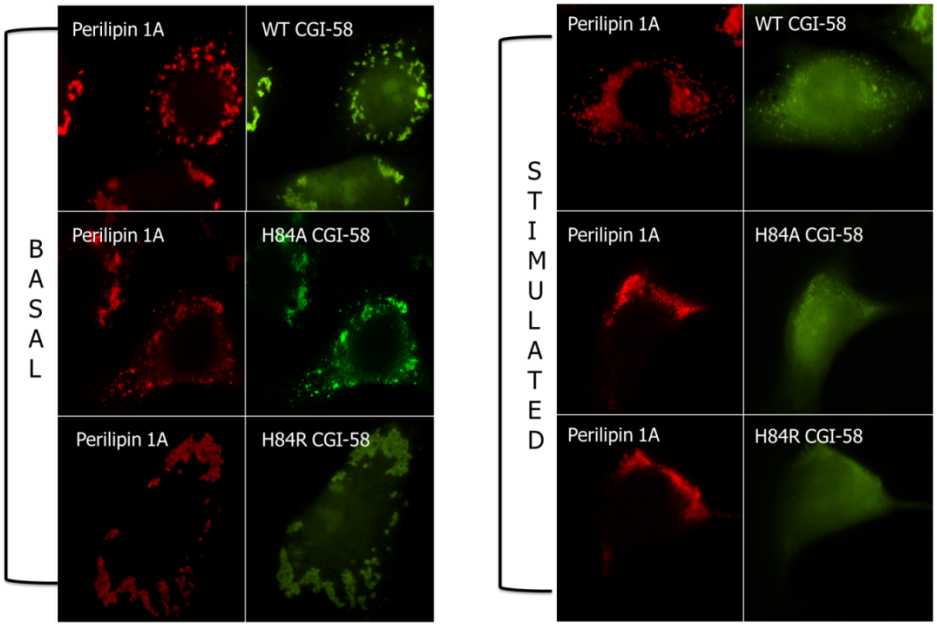
BASAL
STIMULATED
Perilipin 1A
WT CGI-58
Perilipin 1A
H84A CGI-58
Perilipin 1A
H84R CGI-58
Perilipin 1A
WT CGI-58
Perilipin 1A
H84A CGI-58
Perilipin 1A
H84R CGI-58

(B)

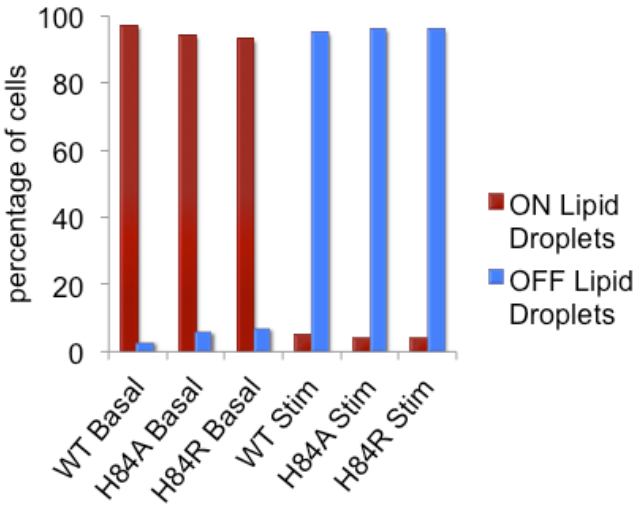
percentage of cells
100
80
60
40
20
0
WT Basal
H84A Basal
H84R Basal
WT Stim
H84A Stim
H84R Stim
ON Lipid Droplets
OFF Lipid Droplets

(C)

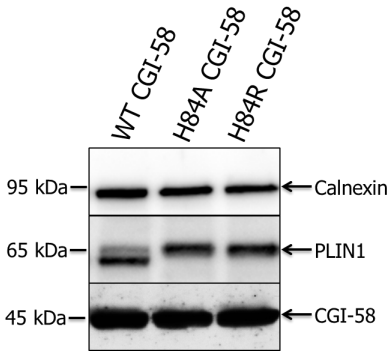
WT CGI-58
H84A CGI-58
H84R CGI-58
95 kDa
65 kDa
45 kDa
Calnexin
PLIN1
CGI-58

Figure 6. Subcellular localization of CGI-58 with H84A or H84R mutations in PLIN1-expressing NIH 3T3 CARΔ fibroblasts

(A) NIH 3T3 CARΔ fibroblasts were transduced with adenoviruses to drive expression of PLIN1 and either WT, H84A, or H84R CGI-58. Cells were lipid loaded with 200 μM oleic acid for 12 hours prior to the addition of forskolin and IBMX for 30 minutes for the stimulation of lipolysis. Basal cells were incubated with DMSO vehicle. Cells were fixed and stained with goat anti-perilipin and rabbit anti-CGI-58 antisera, followed by anti-goat Alexa Fluor 546 (red) and anti-rabbit Alexa Fluor 488 (green) secondary antibodies. Data are from one out of three experiments. (B) Two individuals blinded to sample identity performed cell counts to quantify the subcellular localization of CGI-58 in PLIN1-expressing cells. A minimum of 100 cells were counted for each condition and cells were scored for either a staining pattern representing CGI-58 co-localized with PLIN1 on lipid droplets or a diffuse pattern of CGI-58 staining in the cytoplasm representing CGI-58 dispersed from PLIN1 and off of LDs. Data represent means ± standard error of the mean for cell counts from one experiment out of three. (C) Cell lysate volumes corresponding to 30 μg of total protein were eluted on an SDS-PAGE gel, transferred to a nitrocellulose membrane, and probed with antiserum raised against mouse CGI-58, PLIN1 antiserum, and calnexin antibodies. Cells express comparable normalized protein levels of CGI-58 and PLIN1.

Co-immunoprecipitations of ATGL and CGI-58

We used immunoprecipitations to study CGI-58 binding to ATGL. We first wanted to determine the conditions that promote the best binding of WT CGI-58 to ATGL. We learned from the Zechner group that co-immunoprecipitation of CGI-58 with ATGL works best with co-expression of both proteins in the same cells (R. Zimmermann,privileged correspondence). Thus, we co-expressed both CGI-58 and ATGL in COS-7 cells, and then tested various culture conditions for enhancement of the binding interaction. COS-7 cells ectopically expressing WT CGI-58 and ATGL were incubated under the following conditions prior to harvest of cells for immunoprecipitations: basal (treatment with DMSO vehicle only), stimulated with forskolin and IBMX, basal with prior lipid loading, or stimulated with prior lipid loading (Figure 7). Antiserum raised against CGI-58 or control IgG was used for immunoprecipitations; precipitated proteins were immunoblotted for both CGI-58 and ATGL. WT CGI-58 and ATGL were co-immunoprecipitated with CGI-58 antiserum. In contrast, control IgG did not co-immunoprecipitate WT CGI-58 and ATGL. From these studies, it was clear that neither lipid loading, nor stimulation of cells with forskolin and IBMX is required for the binding interaction of CGI-58 with ATGL. With these data, we decided to use basal conditions when moving forward with the experiments.

To investigate the binding of CGI-58 variants to ATGL, COS-7 cells were co-transduced with both adenoviruses to yield expression of ATGL and one of the CGI-58 variants (Figure 8). Immunoprecipitations used CGI-58 antiserum or control IgG. Immunoblotting of the immunoprecipitated proteins with CGI-58 antiserum revealed the co-immunoprecipitation of ATGL with all variants of CGI-58, suggesting that neither the

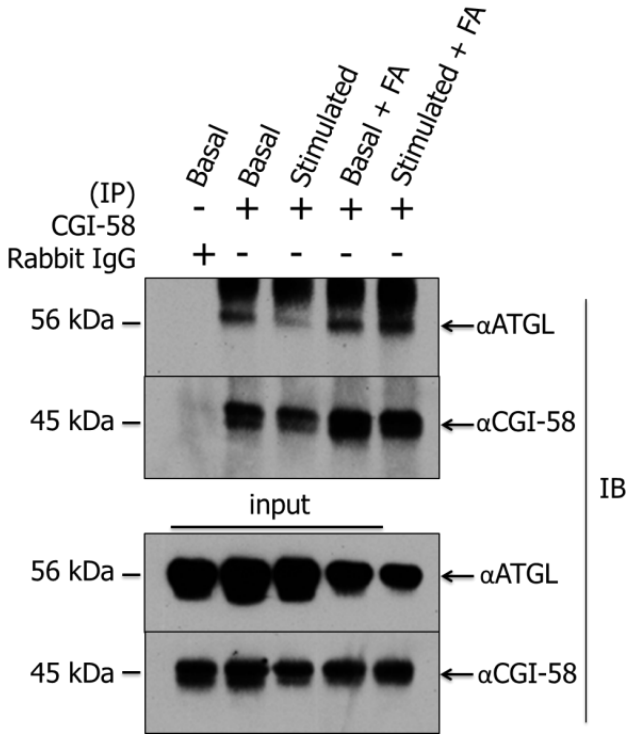

Figure 7. Co-immunoprecipitations of ATGL and WT CGI-58

COS-7 cells ectopically expressing ATGL and WT CGI-58 were either lipid loaded overnight with 400 μM oleic acid (+FA), incubated briefly with isobutylmethylxanthine and forskolin for stimulation of lipolysis (Stimulated), or both (Stimulated + FA). Basal conditions indicate that cells were incubated with DMSO vehicle. Cell extracts (800 μg of total protein) were immunoprecipitated using CGI-58 anti-serum or rabbit IgG (negative control). Proteins were separated by SDS PAGE and immunoblotted for both ATGL and CGI-58. CGI-58 was efficiently precipitated with CGI-58 antiserum; ATGL was detected as a co-immunoprecipitated protein. Stimulation and/or lipid loading of cells did not alter the binding interaction between CGI-58 and ATGL. Neither ATGL nor CGI-58 was detected in immunoprecipitations with control rabbit IgG. The input lanes show the amount of ATGL and CGI-58 in cell extracts (30 μg of total protein). Data are from one out of two experiments.

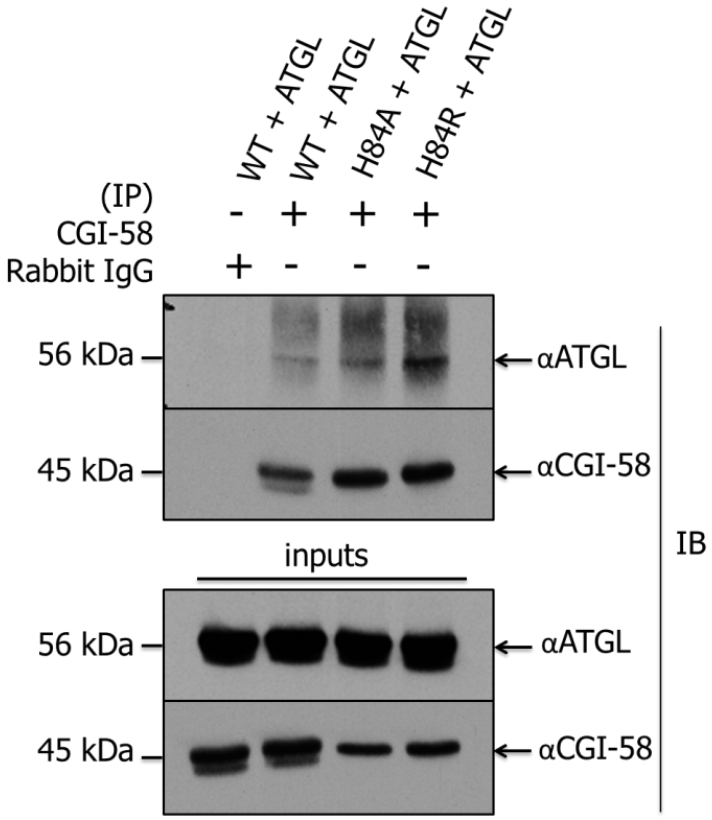

Figure 8. WT CGI-58 and CGI-58 with either an H84A or a H84R mutation bind to ATGL

CGI-58 (WT, H84A, or H84R variants) and ATGL were co-expressed in COS-7 cell extracts prior to immunoprecipitations using CGI-58 antiserum or rabbit IgG (negative control). Proteins were separated on SDS PAGE and immunoblotted for both ATGL and CGI-58. Mutations H84A and H84R did not affect CGI-58 binding to ATGL, since ATGL co-precipitated with both variants. Neither ATGL nor CGI-58 was detected in immunoprecipitations with control rabbit IgG. The input lanes show the amount of ATGL and CGI-58 in cell extracts (30 μg of total protein). Data are from one out of three experiments.

H84A nor the H84R mutation alters CGI-58 binding to ATGL. Interestingly, it was consistently observed in several repetitions of the experiment that H84R CGI-58 and probably also the H84A CGI-58 interacted more strongly with ATGL relative to WT CGI-58.

ATGL and CGI-58 recruitment to lipid droplets

Since the CGI-58 mutations do not reduce the binding of CGI-58 to ATGL, we hypothesized that the reduced function of H84R CGI-58 may be due to reduced recruitment of the protein complex (with ATGL) to LDs, thus reducing ATGL access to substrate lipids. We first assessed the recruitment of ATGL and WT CGI-58 to LDs individually and in combination (Figure 9). COS-7 cells were transduced with WT CGI-58, ATGL, or both WT CGI-58 and ATGL adenoviruses. Lysates of these cells were prepared 48 hours after transduction and were incubated with AD293 cell lysates previously lipid loaded with oleate to make LDs. Lipid droplets were isolated from the combined cell extracts and samples were analyzed by immunoblotting for ATGL and CGI-58. WT CGI-58 was strongly recruited to lipid droplets in both the presence and absence of ATGL. In contrast, ATGL was weakly recruited to lipid droplets in the absence of CGI-58. The presence of CGI-58 increased ATGL recruitment to lipid droplets by 4-fold. These data suggest that CGI-58 plays a role in ATGL recruitment to its lipid substrate.

The same protocol was used to examine binding of the CGI-58 mutated variants to LDs in the presence of ATGL under basal conditions (Figure 10). CGI-58 with either the H84A or the H84R mutation was recruited to LDs with ATGL as effectively as WT CGI-58. COS-7 cell extracts with ectopic ATGL and WT CGI-58 but without LDs, and

uninfected COS-7 cell extracts mixed with LDs were used as negative controls. Neither ATGL nor CGI-58 were detected in LD fractions from the uninfected control lacked CGI-58 and ATGL; thus, there is no detectable endogenous CGI-58 or ATGL and the antibodies did not recognize non-specific proteins. The WT CGI-58 + ATGL (without LDs) control showed that the proteins do not migrate to the top of the gradient during ultracentrifugation in the absence of LDs. These data suggest that the CGI-58 mutations H84A and H84R do not impede the recruitment of CGI-58 with ATGL to LDs.

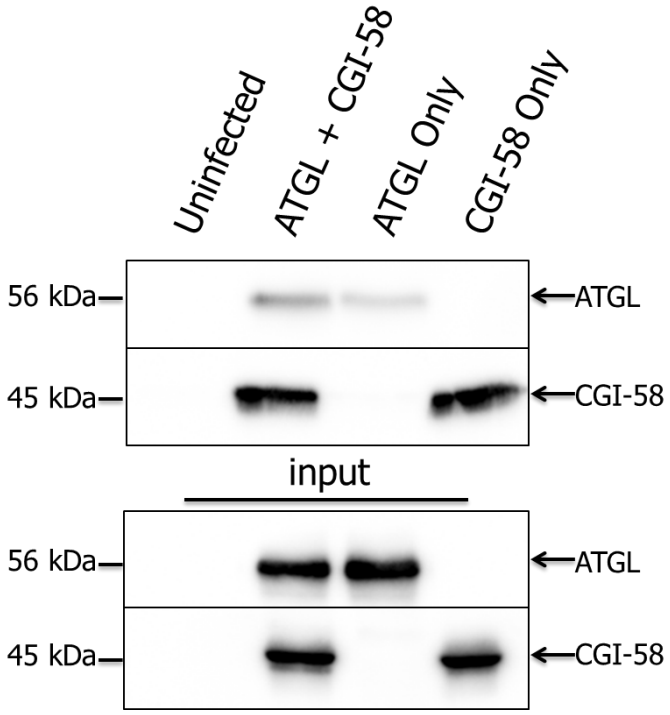

Figure 9. ATGL and WT CGI-58 recruitment to lipid droplets

Lysates of COS-7 cells transduced with ATGL, CGI-58, or both ATGL and CGI-58 adenoviruses were incubated for 1 hour with lysates of AD293 cells previously lipid loaded with 1mM oleate for 20 hours to provide a source of lipid droplets. LDs were isolated by sucrose gradient ultracentrifugation and proteins in the LD fraction were prepared for SDS-PAGE. In the samples used to assess LD binding, ATGL recruitment to lipid droplets was increased by 4-fold with the addition of CGI-58. Volumes corresponding to 40% of the COS-7 lysates were eluted on an SDS-PAGE gel, and proteins were transferred to a nitrocellulose membrane and immunoblotted with CGI-58 antiserum and ATGL antibodies. Input lanes represent 2% of the total COS-7 lysate volume.Both ATGL and CGI-58 are recruited to lipid droplets when tested both individually and in combination; CGI-58 increased the recruitment of ATGL to lipid droplets. These data are from one out of two experiments.

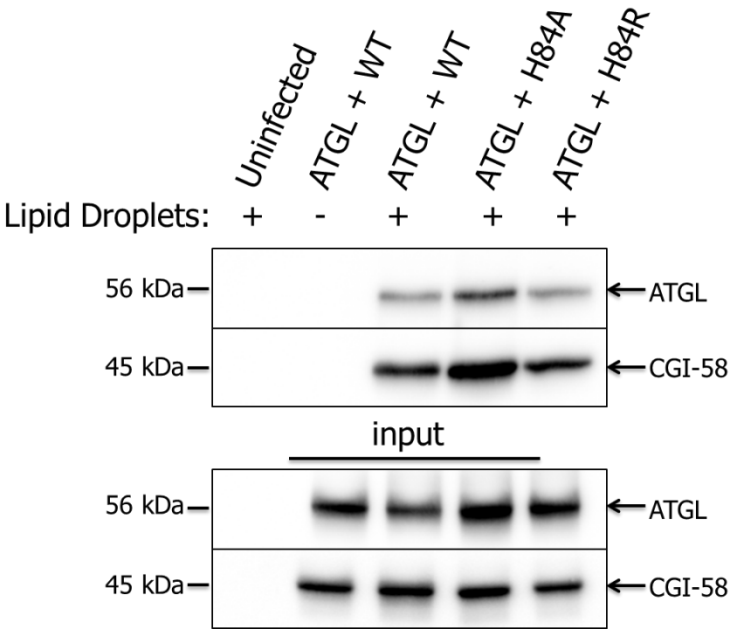

Figure 10. Recruitment of ATGL, WT CGI-58, and CGI-58 with H84A or H84R mutations to lipid droplets

Lysates from COS-7 cells transduced at the same time with both ATGL and one of the CGI-58 variant adenoviruses were incubated with lysates of AD293 cells previously lipid loaded with 1 mM oleate for 20 hours to provide a source of lipid droplets. Lipid droplets were isolated by sucrose gradient ultracentrifugation and proteins were prepared for SDS-PAGE. In samples used to assess LD binding, volumes corresponding to 40% of the COS-7 lysates were eluted on an SDS-PAGE gel, and proteins were transferred to a nitrocellulose membrane, and immunoblotted with CGI-58 antiserum and ATGL antibodies. Input lanes represent 2% of the total COS-7 lysate volume.Neither CGI-58 mutations H84A nor H84R alter recruitment of CGI-58 and ATGL to lipid droplets. CGI-58 with the H84A mutation was more highly recruited to lipid droplets, leading to better recruitment of ATGL to LDs. These data are from one out of three experiments.

DISCUSSION

Our major findings are that H84R CGI-58 fails to co-activate the TAG hydrolase activity of ATGL, while binding ATGL as well as WT CGI-58, and associating with LDs. Furthermore, the H84R mutation does not alter CGI-58 binding to PLIN1 under basal conditions or stimulated release of CGI-58 from PLIN1. To study the importance of histidine 84 in CGI-58 function, we also studied the H84A mutation, and found that it partially co-activates ATGL, suggesting that the histidine residue itself may not be critical to CGI-58 function. Nonetheless, mutation of H84 specifically to an arginine residue significantly impairs CGI-58 function. Thus, our experiments have initiated the characterization of this novel mutation that is observed in humans with NLSDi.

Both H84A and H84R CGI-58 bound to ATGL as well as WT CGI-58, if not better. It is unclear exactly how CGI-58 activates ATGL. If CGI-58 reversibly binds ATGL to increase TAG hydrolysis, and the H84 mutation increases the duration or strength of the binding interaction between the two proteins, then this may be the cause of the significant decrease in ATGL-mediated lipolysis. Perhaps a transient interaction between CGI-58 and ATGL is required for co-activation of TAG hydrolysis. This hypothesis suggests that H84R CGI-58 may sequester ATGL at the surfaces of LDs reducing the efficiency of the release of CGI-58 from ATGL, therefore inhibiting the enzymatic activity of ATGL. Another possibility is that binding of CGI-58 to ATGL may cause a conformational change in either protein that promotes the subsequent release of CGI-58 from ATGL after hydrolysis of a molecule of TAG, in which case, the H84R mutation may alter this conformational change. However, since H84A CGI-58 also

showed increased binding to ATGL, and yet partially retained the function of co-activating ATGL, this mechanism may prove difficult to test.

The findings from this project reveal a novel function of CGI-58. Mixing of lysates from COS-7 cells ectopically expressing CGI-58 or ATGL with a source of LDs resulted in the individual recruitment of each protein to LDs. However, in the presence of CGI-58, ATGL recruitment to LDs increased. Additionally, when there was an increased recruitment of H84A CGI-58 to LDs, ATGL recruitment was consequently increased. It was important to do this experiment in cells lacking PLIN1, since PLIN1 sequestration of CGI-58 would complicate the experiment. We isolated LDs from AD293 cells because there is no endogenous pool of PLIN1; LDs are instead coated with PLIN3 (data not shown), which has never been shown to recruit CGI-58 to LDs. These data suggest that CGI-58 functions to promote ATGL recruitment to LDs. Importantly, we observed that H84R CGI-58 did not impede the recruitment of ATGL to LDs.

It was proposed that CGI-58 could function as an anchor for ATGL binding to LDs (70), but our findings suggest that there is more to the story. The H84R CGI-58 variant is efficient at binding ATGL and is successfully recruited to LDs with ATGL; however, it fails to co-activate ATGL *in vitro* and fails to reduce excess TAG levels in NLSDi human skin fibroblasts. These data support the idea that binding of CGI-58 to ATGL and recruitment of both proteins to lipid substrate is not sufficient for co-activation of ATGL's TAG hydrolase activity and demonstrate that CGI-58 plays an additional role in activating ATGL's enzymatic activity. One possibility is that CGI-58 is needed for hydrolysis of the phospholipid monolayer so that ATGL can gain access to its lipid substrate, in which case, the H84R mutation would reduce phospholipid breakdown.

To test this hypothesis, we would need to analyze phospholipid breakdown *in vitro* by incubating purified WT and H84R CGI-58 with purified ATGL mixed with radiolabeled phospholipids and measuring radioactivity of released fatty acids or phospholipid head groups.

CGI-58 alters the stereochemistry of DAG products of ATGL's TAG hydrolase activity *in vitro.* The Zechner group has shown that incubation of cytosolic fractions of COS-7 cells expressing ATGL with recombinant CGI-58 expands ATGL's hydrolysis of the *sn*-2 fatty acid of TAG to both *sn*-2 and *sn*-1 fatty acids (68). ATGL alone shows preference for hydrolysis of TAG to release only the *sn*-2 fatty acid. The addition of CGI-58 results in the formation of *sn*-1,3 and *sn*-2,3 DAG, with no detectable amount of sn-1,2 DAG. The stereochemical properties of DAG and MAG dictate their biological fate; the product of sn-1 cleavage of TAG (*sn*-2,3 DAG) is not a substrate for phospholipid synthesis, but is a substrate for HSL-mediated hydrolysis. The product of *sn*-2 cleavage of TAG (*sn*-1,3 DAG) is a substrate for re-esterification by diacylglycerol O-acyltransferase 2 (DGAT2) (68). The increase in the regioselectivity of ATGL when co-activated by CGI-58 further suggests that CGI-58 induces a change in ATGL that is more than simply increasing the recruitment of the two proteins to substrate lipids stored in lipid droplets. Perhaps the H84R mutation in CGI-58 alters this function and causes the DAG produced by ATGL-mediated hydrolysis to be limited to *sn*-1,3 DAG, which is then immediately re-esterified into TAG. This can be tested experimentally by inhibiting DGAT2 in NLSDi cells ectopically expressing WT or H84R CGI-58, and then measuring levels of *sn*-1,3 DAG. The mechanism by which CGI-58 modifies ATGL's regioselectivity is still unclear and needs additional work to be elucidated.

Although CGI-58 plays an important role in TAG turnover in cells, it cannot function as a TAG lipase due to the replacement of the typical nucleophilic serine residue in the catalytic triad of α/β hydrolases with an asparagine residue in CGI-58. However, even when asn155 is mutated to serine, CGI-58 still lacks TAG hydrolase activity (79). This suggests that a potential catalytic active site of CGI-58 may be located elsewhere. We hypothesize that histidine H84 may be part of an as yet uncharacterized catalytic active site of CGI-58 that is critical for its function, perhaps through altering the metabolism of phospholipid to reveal the underlying TAG of lipid droplets. However, if this is the case, we would expect the H84A mutated CGI-58 to lack function. H84A CGI-58 was able to reduce excess TAG levels in NLSDi cells as effectively as WT CGI-58, yet co-activation of ATGL's TAG hydrolase activity *in vitro* was reduced relative to WT CGI-58. This reduced co-activation of ATGL's TAG hydrolase activity by H84A CGI-58 was evidently sufficient to reduce excess TAG levels in NLSDi cells.

A small set of amino acid residues are involved in the catalytic activity of an enzyme; understanding the roles of these amino acids in catalysis helps scientists to propose catalytic mechanisms for an enzyme. Histidine and arginine play very different roles in catalytic mechanisms (80), but alanine does not substitute for either function. Histidine is a polar residue that is involved in acid/base catalysis, particularly in proton shuttling. Arginine is mainly involved in electrostatic stabilizing roles and is very rarely involved in proton shuttling. Our data point to an important role for the amino acid in position 84 in either the structure or function of CGI-58, but also suggest that histidine in this position probably does not serve a role in proton donation, since alanine can replace H84 without eliminating CGI-58 activity. Additionally, the potential stabilizing role of

arginine in position 84 is inhibitory to CGI-58's function through an as yet unknown mechanism.

The crystal structure of CGI-58 is not yet available, so a member of our group, Daniel Kurz, created a hypothetical 3D model of CGI-58 protein structure to better understand the spatial positioning of proposed active site residues (Figure 11). The highest ranked model was based on the crystal structure of a hydrolase from *Bacillus subtilis* (Protein Data Bank ID: 2R11). The full 352-amino acid sequence for mouse CGI-58 (NP_080455.1) was used to generate the model using the online Protein Homology/analogy Recognition Engine (PHYRE) version 0.2 software; the model image was generated using The PyMOL Molecular Graphics System, Version 1.5.0.1 Schrödinger, LLC. Using this model, we located an aspartate residue at position 110 in CGI-58 in close proximity to H84; both residues are located in a hydrophobic pocket in the protein. If H84 serves a catalytic function, then D110 could be the acidic component of a catalytic active site. To test this, several experiments could be done. A D110A mutated variant of CGI-58 could be expressed in NLSDi fibroblasts followed by analysis of TAG content to test the importance of this residue in TAG turnover. Additionally, the recombinant D110A variant can be tested for co-activation of ATGL's TAG hydrolase activity in the *in vitro* assay. We initiated the latter experiments, but found that D110A was poorly expressed in *E. coli* and difficult to purify. If D110A CGI-58 lacks the capacity to increase either ATGL activity *in vitro* or TAG turnover in NLSDi cells, then these observations may support the idea that H84 and D110 are catalytic residues. The remaining question is, for what activity?

The general goal of this project was to characterize the H84R mutation in mouse

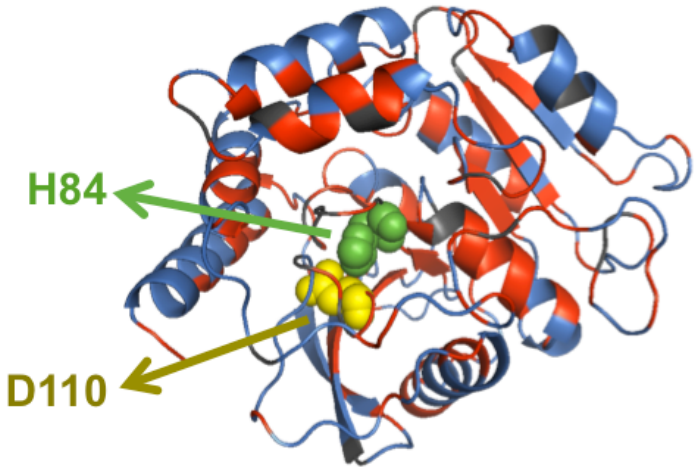

Figure 11. Proposed catalytic active site of CGI-58

Residues H84 and D110 are putative active site residues. Both residues are located in a hydrophobic pocket of the protein and are in close proximity to each other (model developed by Daniel Kurz).

CGI-58 to elucidate mechanisms responsible for CGI-58 function and to gain understanding of why the H82R mutation causes NLSDi in humans. CGI-58 is known to co-activate ATGL (12), but when comparing the different phenotypes of patients with NLSDm and NLSDi, it becomes apparent that CGI-58 functions independently of ATGL in an additional mechanism that is currently unknown (11,64). Patients with NLSDi have severe ichthyosis, which is not present in patients with NLSDm (11,61,64). Additionally, ATGL deletion from mice induces TAG accumulation in multiple tissues and cardiomyopathy leading to death in early adulthood (49), while CGI-58 deletion from mice causes a lethal skin barrier defect resulting in death soon after birth (66). These observations led researchers to propose that CGI-58 has a separate function from ATGL

in skin cells. Additionally, phospholipid synthesis from DAG is impaired in NLSDi fibroblasts suggesting that CGI-58 might play a role in the provision of DAG from TAG hydrolysis to phospholipid biosynthetic enzymes (10,81). The use of antisense oligonucleotides to silence CGI-58 in the liver and adipose tissue of mice resulted in decreased fat mass and protection against high fat-induced obesity (82), contrasting with the increased fat mass observed in ATGL-null mice (49). Thus, it is clear that CGI-58's functions in lipid homeostasis are incompletely understood and include mechanisms distinct from co-activation of ATGL.

Examining the association of CGI-58 and PLIN1 is important to gain understanding of the compartmentalization and consequent control of activity of CGI-58 in adipose tissue, however, PLIN1 is not expressed in all cells. More specifically, PLIN1 is not expressed in skin cells or hepatocytes, where patients with NLSDi exhibit severe problems in TAG metabolism. These data indicate that CGI-58 plays an additional and perhaps more crucial role in the skin and liver.

Overall, several questions remain: How does CGI-58 co-activate ATGL, what is the ATGL-independent function of CGI-58, and how does the H84R mutation alter CGI-58 function? Our findings begin the characterization of the H82R mutation in CGI-58 that causes NLSDi in humans. Further investigation is needed to determine the mechanism responsible for dysfunction of H82R CGI-58 and the mechanism by which WT CGI-58 co-activates ATGL.

REFERENCES

1. Ogden CL, Carroll MD, Kit BK, Flegal KM. Prevalence of childhood and adult obesity in the United States, 2011-2012. JAMA. American Medical Association; 2014 Feb 26;806–14.
2. Wolf AM, Colditz GA. Current estimates of the economic cost of obesity in the United States. Obes Res. 1998 Mar;97–106.
3. Guo Y, Cordes KR, Farese R V, Walther TC. Lipid droplets at a glance. J Cell Sci. 2009 Mar 15;749–52.
4. Blanchette-Mackie E, Dwyer N, Barber T, Coxey R, Takeda T, Rondinone C, Theodorakis J, Greenberg A, Londos C. Perilipin is located on the surface layer of intracellular lipid droplets in adipocytes. J Lipid Res. 1995 Jun;1211–26.
5. Brasaemle DL. Lipolysis control: the plot thickens. Cell Metab. Elsevier Inc.; 2010 Mar 3;173–4.
6. Frühbeck G, Méndez-Giménez L, Fernández-Formoso J-A, Fernández S, Rodríguez A. Regulation of adipocyte lipolysis. Nutrition research reviews. 2014.
7. Taylor SS, Yang J, Wu J, Haste NM, Radzio-Andzelm E, Anand G. PKA: a portrait of protein kinase dynamics. Biochim Biophys Acta. 2004 Mar 11;259–69.
8. Honnor RC, Dhillon GS, Londoss C. CAMP-dependent Protein Kinase and Lipolysis in Rat Adipocytes 11. J Biol Chem. 1984;15130–8.
9. Lafontan M, Langin D. Lipolysis and lipid mobilization in human adipose tissue. Prog Lipid Res. 2009 Sep;275–97.
10. Igal RA, Coleman RA. Acylglycerol Recycling from Triacylglycerol to Phospholipid, Not Lipase Activity, Is Defective in Neutral Lipid Storage Disease Fibroblasts. J Biol Chem. 1996;16644–51.
11. Lefèvre C, Jobard F, Caux F, Bouadjar B, Karaduman A, Heilig R, Lakhdar H, Wollenberg A, Verret JL, Weissenbach J, Ozgüc M, Lathrop M, Prud'homme JF, Fischer J. Mutations in CGI-58, the gene encoding a new protein of the esterase/lipase/thioesterase subfamily, in Chanarin-Dorfman syndrome. Am J Hum Genet. 2001 Nov;1002–12.
12. Lass A, Zimmermann R, Haemmerle G, Riederer M, Schoiswohl G, Schweiger M, Kienesberger P, Strauss JG, Gorkiewicz G, Zechner R. Adipose triglyceride lipase-mediated lipolysis of cellular fat stores is activated by CGI-58 and defective in Chanarin-Dorfman Syndrome. Cell Metab. 2006 May;309–19.
13. Greenberg AS, Egan JJ, Wek SA, Garty NB, Blanchette-Mackie EJ, Londos C. Perilipin, a major hormonally regulated adipocyte-specific phosphoprotein associated with the periphery of lipid storage droplets. J Biol Chem. 1991 Jun 15;11341–6.
14. Jiang HP, Serrero G. Isolation and characterization of a full-length cDNA coding for an adipose differentiation-related protein. Proc Natl Acad Sci U S A. 1992 Sep 1;7856–60.
15. Wolins NE, Quaynor BK, Skinner JR, Tzekov A, Croce MA, Gropler MC, Varma V, Yao-Borengasser A, Rasouli N, Kern PA, Finck BN, Bickel PE. OXPAT/PAT-1 is a PPAR-induced lipid droplet protein that promotes fatty acid utilization. Diabetes. 2006 Dec;3418–28.

16. Díaz E, Pfeffer SR. TIP47: a cargo selection device for mannose 6-phosphate receptor trafficking. Cell. 1998 May 1;433–43.
17. Scherer PE, Bickel PE, Kotler M, Lodish HF. Cloning of cell-specific secreted and surface proteins by subtractive antibody screening. Nat Biotechnol. 1998 Jun;581–6.
18. Brasaemle D, Rubin B, Harten I, Gruia-Gray J, Kimmel A, Londos C. Perilipin A increases triacylglycerol storage by decreasing the rate of triacylglycerol hydrolysis. J Biol Chem. 2000 Dec 8;38486–93.
19. Servetnick DA, Brasaemle DL, Gruia-Gray J, Kimmel AR, Wolff J, Londos C. Perilipins are associated with cholesteryl ester droplets in steroidogenic adrenal cortical and Leydig cells. J Biol Chem. 1995 Jul 14;16970–3.
20. Martinez-Botas J, Anderson JB, Tessier D, Lapillonne A, Chang BH, Quast MJ, Gorenstein D, Chen KH, Chan L. Absence of perilipin results in leanness and reverses obesity in Lepr(db/db) mice. Nat Genet. 2000 Dec;474–9.
21. Tansey JT, Sztalryd C, Gruia-Gray J, Roush DL, Zee J V, Gavrilova O, Reitman ML, Deng CX, Li C, Kimmel AR, Londos C. Perilipin ablation results in a lean mouse with aberrant adipocyte lipolysis, enhanced leptin production, and resistance to diet-induced obesity. Proc Natl Acad Sci U S A. 2001 May 22;6494–9.
22. Brasaemle DL. Thematic review series: adipocyte biology. The perilipin family of structural lipid droplet proteins: stabilization of lipid droplets and control of lipolysis. J Lipid Res. 2007 Dec;2547–59.
23. Sztalryd C, Xu G, Dorward H, Tansey JT, Contreras JA, Kimmel AR, Londos C. Perilipin A is essential for the translocation of hormone-sensitive lipase during lipolytic activation. J Cell Biol. 2003 Jun 23;1093–103.
24. Wang H, Hu L, Dalen K, Dorward H, Marcinkiewicz A, Russell D, Gong D, Londos C, Yamaguchi T, Holm C, Rizzo M a, Brasaemle D, Sztalryd C. Activation of hormone-sensitive lipase requires two steps, protein phosphorylation and binding to the PAT-1 domain of lipid droplet coat proteins. J Biol Chem. 2009 Nov 13;32116–25.
25. Zhang HH, Souza SC, Muliro K V, Kraemer FB, Obin MS, Greenberg AS. Lipase-selective functional domains of perilipin A differentially regulate constitutive and protein kinase A-stimulated lipolysis. J Biol Chem. 2003 Dec 19;51535–42.
26. Subramanian V, Rothenberg A, Gomez C, Cohen AW, Garcia A, Bhattacharyya S, Shapiro L, Dolios G, Wang R, Lisanti MP, Brasaemle DL. Perilipin A mediates the reversible binding of CGI-58 to lipid droplets in 3T3-L1 adipocytes. J Biol Chem. 2004 Oct 1;42062–71.
27. Kraemer FB, Patel S, Saedi MS, Sztalryd C. Detection of hormone-sensitive lipase in various tissues. I. Expression of an HSL/bacterial fusion protein and generation of anti-HSL antibodies. J Lipid Res. 1993 Apr;663–71.
28. Khoo JC, Reue K, Steinberg D, Schotz MC. Expression of hormone-sensitive lipase mRNA in macrophages. J Lipid Res. 1993 Nov;1969–74.
29. Holm C, Kirchgessner TG, Svenson KL, Fredrikson G, Nilsson S, Miller CG, Shively JE, Heinzmann C, Sparkes RS, Mohandas T. Hormone-sensitive lipase: sequence, expression, and chromosomal localization to 19 cent-q13.3. Science. 1988 Sep 16;1503–6.

30. Small CA, Garton AJ, Yeaman SJ. The presence and role of hormone-sensitive lipase in heart muscle. Biochem J. 1989 Feb 15;67–72.
31. Langfort J, Ploug T, Ihlemann J, Enevoldsen LH, Stallknecht B, Saldo M, Kjaer M, Holm C, Galbo H. Hormone-sensitive lipase (HSL) expression and regulation in skeletal muscle. Adv Exp Med Biol. 1998 Jan;219–28.
32. Jepson CA, Yeaman SJ. Expression of hormone-sensitive lipase in macrophage foam cells. Biochem Soc Trans. 1993 Aug;232S.
33. Fredrikson G, Strålfors P, Nilsson N, Belfrage P. Hormone-sensitive lipase of rat adipose tissue. Purification and some properties. J Biol Chem. 1981 Jun 25;6311–20.
34. Wei S, Lai K, Patel S, Piantedosi R, Shen H, Colantuoni V, Kraemer FB, Blaner WS. Retinyl ester hydrolysis and retinol efflux from BFC-1beta adipocytes. J Biol Chem. 1997 May 30;14159–65.
35. Haemmerle G, Zimmermann R, Hayn M, Theussl C, Waeg G, Wagner E, Sattler W, Magin TM, Wagner EF, Zechner R. Hormone-sensitive lipase deficiency in mice causes diglyceride accumulation in adipose tissue, muscle, and testis. J Biol Chem. 2002 Feb 15;4806–15.
36. Shakur Y, Holst LS, Landstrom TR, Movsesian M, Degerman E, Manganiello V. Regulation and function of the cyclic nucleotide phosphodiesterase (PDE3) gene family. Prog Nucleic Acid Res Mol Biol. 2001 Jan;241–77.
37. Workman P. Inhibiting the phosphoinositide 3-kinase pathway for cancer treatment. Biochem Soc Trans. 2004 Apr;393–6.
38. Garton AJ, Campbell DG, Carling D, Hardie DG, Colbran RJ, Yeaman SJ. Phosphorylation of bovine hormone-sensitive lipase by the AMP-activated protein kinase. A possible antilipolytic mechanism. Eur J Biochem. 1989 Jan 15;249–54.
39. Daval M, Diot-Dupuy F, Bazin R, Hainault I, Viollet B, Vaulont S, Hajduch E, Ferré P, Foufelle F. Anti-lipolytic action of AMP-activated protein kinase in rodent adipocytes. J Biol Chem. 2005 Jul 1;25250–7.
40. Su C-L, Sztalryd C, Contreras JA, Holm C, Kimmel AR, Londos C. Mutational analysis of the hormone-sensitive lipase translocation reaction in adipocytes. J Biol Chem. 2003 Oct 31;43615–9.
41. Anthonsen MW, Rönnstrand L, Wernstedt C, Degerman E, Holm C. Identification of novel phosphorylation sites in hormone-sensitive lipase that are phosphorylated in response to isoproterenol and govern activation properties in vitro. J Biol Chem. 1998 Jan 2;215–21.
42. Brasaemle DL, Levin DM, Adler-Wailes DC, Londos C. The lipolytic stimulation of 3T3-L1 adipocytes promotes the translocation of hormone-sensitive lipase to the surfaces of lipid storage droplets. Biochim Biophys Acta - Mol Cell Biol Lipids. 2000 Jan;251–62.
43. Osuga J, Ishibashi S, Oka T, Yagyu H, Tozawa R, Fujimoto A, Shionoiri F, Yahagi N, Kraemer FB, Tsutsumi O, Yamada N. Targeted disruption of hormone-sensitive lipase results in male sterility and adipocyte hypertrophy, but not in obesity. Proc Natl Acad Sci U S A. 2000 Jan 18;787–92.
44. Wang SP, Laurin N, Himms-Hagen J, Rudnicki MA, Levy E, Robert MF, Pan L, Oligny L, Mitchell GA. The adipose tissue phenotype of hormone-sensitive lipase deficiency in mice. Obes Res. 2001 Feb;119–28.

45. Jenkins CM, Mancuso DJ, Yan W, Sims HF, Gibson B, Gross RW. Identification, cloning, expression, and purification of three novel human calcium-independent phospholipase A2 family members possessing triacylglycerol lipase and acylglycerol transacylase activities. J Biol Chem. 2004 Nov 19;48968–75.
46. Villena JA, Roy S, Sarkadi-Nagy E, Kim K-H, Sul HS. Desnutrin, an adipocyte gene encoding a novel patatin domain-containing protein, is induced by fasting and glucocorticoids: ectopic expression of desnutrin increases triglyceride hydrolysis. J Biol Chem. 2004 Nov 5;47066–75.
47. Zimmermann R, Strauss JG, Haemmerle G, Schoiswohl G, Birner-Gruenberger R, Riederer M, Lass A, Neuberger G, Eisenhaber F, Hermetter A, Zechner R. Fat mobilization in adipose tissue is promoted by adipose triglyceride lipase. Science (80-). 2004 Nov 19;1383–6.
48. Lake AC, Sun Y, Li J-L, Kim JE, Johnson JW, Li D, Revett T, Shih HH, Liu W, Paulsen JE, Gimeno RE. Expression, regulation, and triglyceride hydrolase activity of Adiponutrin family members. J Lipid Res. 2005 Nov;2477–87.
49. Haemmerle G, Lass A, Zimmermann R, Gorkiewicz G, Meyer C, Rozman J, Heldmaier G, Maier R, Theussl C, Eder S, Kratky D, Wagner EF, Klingenspor M, Hoefler G, Zechner R. Defective lipolysis and altered energy metabolism in mice lacking adipose triglyceride lipase. Science. 2006 May 5;734–7.
50. Zechner R, Kienesberger PC, Haemmerle G, Zimmermann R, Lass A. Adipose triglyceride lipase and the lipolytic catabolism of cellular fat stores. J Lipid Res. 2009 Jan;3–21.
51. Pagnon J, Matzaris M, Stark R, Meex RCR, Macaulay SL, Brown W, O'Brien PE, Tiganis T, Watt MJ. Identification and functional characterization of protein kinase A phosphorylation sites in the major lipolytic protein, adipose triglyceride lipase. Endocrinology. Endocrine Society Chevy Chase, MD; 2012 Sep 25;4278–89.
52. Ahmadian M, Abbott MJ, Tang T, Hudak CSS, Kim Y, Bruss M, Hellerstein MK, Lee H-Y, Samuel VT, Shulman GI, Wang Y, Duncan RE, Kang C, Sul HS. Desnutrin/ATGL is regulated by AMPK and is required for a brown adipose phenotype. Cell Metab. 2011 Jun 8;739–48.
53. Yang X, Lu X, Lombès M, Rha GB, Chi Y-I, Guerin TM, Smart EJ, Liu J. The G(0)/G(1) switch gene 2 regulates adipose lipolysis through association with adipose triglyceride lipase. Cell Metab. 2010 Mar 3;194–205.
54. Soni KG, Mardones GA, Sougrat R, Smirnova E, Jackson CL, Bonifacino JS. Coatomer-dependent protein delivery to lipid droplets. J Cell Sci. 2009 Jun 1;1834–41.
55. Lu X, Yang X, Liu J. Differential control of ATGL-mediated lipid droplet degradation by CGI-58 and G0S2. Cell Cycle. 2010 Jul 15;2791–7.
56. Schweiger M, Paar M, Eder C, Brandis J, Moser E, Gorkiewicz G, Grond S, Radner FPW, Cerk I, Cornaciu I, Oberer M, Kersten S, Zechner R, Zimmermann R, Lass A. G0/G1 switch gene-2 regulates human adipocyte lipolysis by affecting activity and localization of adipose triglyceride lipase. J Lipid Res. 2012 Nov;2307–17.
57. Lai CH, Chou CY, Ch'ang LY, Liu CS, Lin W. Identification of novel human genes evolutionarily conserved in Caenorhabditis elegans by comparative proteomics. Genome Res. 2000 May;703–13.

58. Dorfman ML. Ichthyosiform Dermatosis With Systemic Lipidosis. Arch Dermatol. American Medical Association; 1974 Aug 1;261.
59. Chanarin I, Patel A, Slavin G, Wills EJ, Andrews TM, Stewart G. Neutral-lipid storage disease: a new disorder of lipid metabolism. Br Med J. 1975 Mar 8;553–5.
60. Slavin G, Wills EJ, Richmond JE, Chanarin I, Andrews T, Stewart G. Morphological features in a neutral lipid storage disease. J Clin Pathol. 1975 Sep;701–10.
61. Igal R, Rhoads J, Coleman R. Neutral lipid storage disease with fatty liver and cholestasis. J Pediatr Gastroenterol Nutr. 1997 Nov;541–7.
62. Bruno C, Bertini E, Di Rocco M, Cassandrini D, Ruffa G, De Toni T, Seri M, Spada M, Li Volti G, D'Amico A, Trucco F, Arca M, Casali C, Angelini C, Dimauro S, Minetti C. Clinical and genetic characterization of Chanarin-Dorfman syndrome. Biochem Biophys Res Commun. 2008 May 16;1125–8.
63. Schweiger M, Lass A, Zimmermann R, Eichmann TO, Zechner R. Neutral lipid storage disease : genetic disorders caused by mutations in adipose triglyceride lipase / PNPLA2 or CGI-58 / ABHD5. Am J Physiol Endocrinol Metab. 2009;E289–E296.
64. Fischer J, Lefèvre C, Morava E, Mussini J-M, Laforêt P, Negre-Salvayre A, Lathrop M, Salvayre R. The gene encoding adipose triglyceride lipase (PNPLA2) is mutated in neutral lipid storage disease with myopathy. Nat Genet. 2007 Jan;28–30.
65. Granneman JG, Moore H-PH, Krishnamoorthy R, Rathod M. Perilipin controls lipolysis by regulating the interactions of AB-hydrolase containing 5 (Abhd5) and adipose triglyceride lipase (Atgl). J Biol Chem. 2009 Dec 11;34538–44.
66. Radner FPW, Streith IE, Schoiswohl G, Schweiger M, Kumari M, Eichmann TO, Rechberger G, Koefeler HC, Eder S, Schauer S, Theussl HC, Preiss-Landl K, Lass A, Zimmermann R, Hoefler G, Zechner R, Haemmerle G. Growth retardation, impaired triacylglycerol catabolism, hepatic steatosis, and lethal skin barrier defect in mice lacking comparative gene identification-58 (CGI-58). J Biol Chem. 2010 Mar 5;7300–11.
67. Schleinitz N, Fischer J, Sanchez A, Veit V, Harle J-R, Pelissier J-F. Two New Mutations of the ABHD5 Gene in a New Adult Case of Chanarin Dorfman Syndrome: An Uncommon Lipid Storage Disease. Arch Derm. 2005;798–800.
68. Eichmann TO, Kumari M, Haas JT, Farese R V, Zimmermann R, Lass A, Zechner R. Studies on the substrate and stereo/regioselectivity of adipose triglyceride lipase, hormone-sensitive lipase, and diacylglycerol-O-acyltransferases. J Biol Chem. 2012 Nov 30;41446–57.
69. Cornaciu I, Boeszoermenyi A, Lindermuth H, Nagy HM, Cerk IK, Ebner C, Salzburger B, Gruber A, Schweiger M, Zechner R, Lass A, Zimmermann R, Oberer M. The minimal domain of adipose triglyceride lipase (ATGL) ranges until leucine 254 and can be activated and inhibited by CGI-58 and G0S2, respectively. PLoS One. 2011 Jan;e26349.
70. Gruber A, Cornaciu I, Lass A, Schweiger M, Poeschl M, Eder C, Kumari M, Schoiswohl G, Wolinski H, Kohlwein SD, Zechner R, Zimmermann R, Oberer M. The N-terminal region of comparative gene identification-58 (CGI-58) is

important for lipid droplet binding and activation of adipose triglyceride lipase. J Biol Chem. 2010 Apr 16;12289–98.
71. Wang H, Bell M, Sreenivasan U, Sreenevasan U, Hu H, Liu J, Dalen K, Londos C, Yamaguchi T, Rizzo M a, Coleman R, Gong D, Brasaemle D, Sztalryd C. Unique regulation of adipose triglyceride lipase (ATGL) by perilipin 5, a lipid droplet-associated protein. J Biol Chem. 2011 May 6;15707–15.
72. Tornqvist H, Belfrage P. Purification hydrolyzing and Some Properties of a Monoacylglycerol- Enzyme of Rat Adipose Tissue. J Biol Chem. 1976;813–9.
73. Brasaemle DL, Barber T, Wolins NE, Serrero G, Blanchette-Mackie EJ, Londos C. Adipose differentiation-related protein is an ubiquitously expressed lipid storage droplet-associated protein. J Lipid Res. 1997 Nov;2249–63.
74. Lampidonis AD, Rogdakis E, Voutsinas GE, Stravopodis DJ. The resurgence of Hormone-Sensitive Lipase (HSL) in mammalian lipolysis. Gene. 2011 May 15;1–11.
75. Orlicky DJ, DeGregori J, Schaack J. Construction of stable coxsackievirus and adenovirus receptor-expressing 3T3-L1 cells. J Lipid Res. 2001 Jun 1;910–5.
76. Jager L, Hausl MA, Rauschhuber C, Wolf NM, Kay MA, Ehrhardt A. A rapid protocol for construction and production of high-capacity adenoviral vectors. Nat Protoc. 2009 Jan;547–64.
77. Laemmli UK. Cleavage of structural proteins during the assembly of the head of bacteriophage T4. Nature. 1970 Aug 15;680–5.
78. Schwartz DM, Wolins NE. A simple and rapid method to assay triacylglycerol in cells and tissues. J Lipid Res. 2007 Nov;2514–20.
79. Lass A, Zimmermann R, Oberer M, Zechner R. Lipolysis - a highly regulated multi-enzyme complex mediates the catabolism of cellular fat stores. Prog Lipid Res. 2011 Jan;14–27.
80. Holliday GL, Mitchell JBO, Thornton JM. Understanding the functional roles of amino acid residues in enzyme catalysis. J Mol Biol. Elsevier Ltd; 2009 Jul 17;560–77.
81. Igal R, Coleman R. Neutral lipid storage disease: a genetic disorder with abnormalities in the regulation of phospholipid metabolism. J Lipid Res. 1998 Jan;31–43.
82. Brown JM, Betters JL, Lord C, Ma Y, Han X, Yang K, et al. CGI-58 knockdown in mice causes hepatic steatosis but prevents diet-induced obesity and glucose intolerance. J Lipid Res. 2010 Nov;3306–15.